Build Simul (2022) 15: 1747–1773
https://doi.org/10.1007/s12273-022-0895-y

Intelligent windows for electricity generation: A technologies review

Manlio Salas Castillo[1], Xiao Liu[1], Fedaa Abd-AlHamid[2], Karen Connelly[1], Yupeng Wu[1] (✉)

1. Department of Architecture and Built Environment, Faculty of Engineering, University of Nottingham, University Park, Nottingham, NG7 2RD, UK

2. Department of Architecture, Faculty of Architecture and Design, Al-Zaytoonah University of Jordan, Amman, Jordan

Review Article

Abstract

Buildings are responsible for over 40% of total primary energy consumption in the US and EU and therefore improving building energy efficiency has significant potential for obtaining net-zero energy buildings reducing energy consumption. The concurrent demands of environmental comfort and the need to improve energy efficiency for both new and existing buildings have motivated research into finding solutions for the regulation of incoming solar radiation, as well as ensuring occupant thermal and visual comfort whilst generating energy onsite. Windows as building components offer the opportunity of addressing these issues in buildings. Building integration of photovoltaics permits building components such as semi-transparent façade, skylights and shading devices to be replaced with PV. Much progress has been made in photovoltaic material science, where smart window development has evolved in areas such as semi-transparent PV, electrochromic and thermochromic materials, luminescent solar concentrator and the integration of each of the latter technologies to buildings, specifically windows. This paper presents a review on intelligent window technologies that integrate renewable energy technologies with energy-saving strategies contributing potential solutions towards sustainable zero-energy buildings. This review is a comprehensive evaluation of intelligent windows focusing on state-of-the-art development in windows that can generate electricity and their electrical, thermal and optical characteristics. This review provides a summary of current work in intelligent window design for energy generation and gives recommendations for further research opportunities.

Keywords

intelligent window;
electricity generation;
photovoltaic;
building integrated PV;
solar concentrator;
electricity-generating smart window

Article History

Received: 22 October 2021
Revised: 18 February 2022
Accepted: 02 March 2022

1 Introduction

In recent years, the search for innovative ways to improve energy consumption is becoming increasingly popular. In countries like the US and China, buildings currently account for over 41% and 28% of total energy consumption, respectively (Xia et al. 2014). Energy usage in buildings is largely required for creating a thermally and visually comfortable environment for building occupants through the use of ventilation, heating, cooling and artificial lighting services which are typically responsible for over 70% of total energy demand in buildings (Abdallah et al. 2015; Ruparathna et al. 2016). Amongst the building components, windows have a considerable impact on energy consumption and the indoor environment. Optimum window design and glazing could reduce residential building energy consumption by 10% to 50% in most climates. Additionally, for commercial, institutional and industrial buildings, a properly specified fenestration system could reduce lighting and air-conditioning costs by 10% to 40% (Cuce et al. 2015; Cuce and Riffat 2015; Ihara et al. 2015; Vanhoutteghem et al. 2015; Gorgolis and Karamanis 2016; Mangkuto et al. 2016). Significant reductions in thermal transmittance, or *U*-value, of fenestration products, are achieved through the use of multiple glass panes enclosing air or inert gas to reduce conduction and convection, and low emissivity coatings on the glass surfaces to reduce long-wave heat exchange (Jelle et al. 2012a). Strategies to manipulate glazing spectral response also have been developed, the simplest of which can introduce tint to the glass to absorb radiation or apply thin film coatings to reflect radiation (Jelle et al. 2012a; Manasrah et al. 2021). Smart windows designed to regulate the amount

E-mail: Yupeng.Wu@nottingham.ac.uk

Building Systems and Components

List of symbols

A	collector aperture area	T_{in}	coolant temperature inlet
C	specific heat capacity of the coolant	T_{out}	coolant temperature outlet
C_g	geometric concentration ratio	V_{mpp}	voltage at maximum power operation
G	incident solar irradiance	V_{oc}	open circuit voltage
I_{mpp}	electric current at maximum power operation	η_e	electrical efficiency
J_{sc}	short circuit current	η_t	thermal efficiency
P_{max}	maximum power point	θ_c	nominal half acceptance angle
$\dot{m}$	mass flow rate		

of transmitted solar and long-wave radiation in response to an applied stimulus such as heat (thermochromism), electricity (electrochromism) and light (photochromism), have demonstrated significant potential for buildings' energy consumption reduction (Nitz and Hartwig 2005; Cuce and Riffat 2015; Gorgolis and Karamanis 2016). In addition, windows can also be used for electricity generation when integrated with PV systems. Aside from offering aesthetically pleasing features to buildings along with energy generation, these PV systems can act as blinds to protect from direct sunlight, therefore, reducing air conditioning loads.

Within this work, a review of the current windows' technologies for electricity generation is provided. It includes the traditional building integration of PV systems for glazing façades and windows and their components applications and investigates the different types of solar cells suitable for these applications, e.g., Si, thin-film, organic and dye-sensitized solar cells. The thermal, optical and electrical performance for building-integrated PV systems along with their effects on building performance are discussed. In addition, complex systems such as solar thermal PV windows, building integrated concentrating PV windows including organic dyes and quantum dots based luminescent solar concentrator (LSC) windows are also reviewed. Finally, recent research on smart window integrated PV systems that are suitable for electricity generation and dynamically control the solar radiation entering the indoor space through the window systems is introduced. Overall this review paper aims to provide a comprehensive overview of the potential impact of the integration of smart window technologies on the energy efficiency of buildings.

2 Building integrated PV (BIPV) systems

2.1 Overview of PV technologies for building integration

Traditionally, PV power plants needed to be situated where there are extensive areas of land and therefore, have been located outside cities requiring long transmission lines (cable) to reach load centres (Ikkurti and Saha 2015). This can be avoided by integrating PV directly into or mounting onto, buildings i.e., building integrated PV (BIPV). Aside from the inherent power generation function of BIPV systems, they can also be beneficial in substituting some of the building components, e.g., the façades, windows, or shading devices (Fossa et al. 2008). Hence, BIPVs may provide savings in materials and labour, as well as reducing electricity costs, therefore, providing additional economic benefits for the building envelope (Jelle and Breivik 2012). It is also becoming increasingly popular to integrate PV into building windows or glazed façades to offer aesthetically pleasing features to buildings (Makrides et al. 2010).

Most types of PV technologies illustrated in Figure 1 are adaptable to windows. The crystalline silicon (c-Si) solar cells can reach an efficiency of approximately 22% (ITRPV 2014), and the market share of the c-Si is around 90% by 2017(ITRPV 2018). Gallium arsenide (GaAs) solar cells offer low non-radiative energy loss, high absorption, direct bandgap with the solar spectrum (ITRPV 2014) and 24%–28% efficiency (Kayes et al. 2011; Mattos et al. 2012). However, high manufacturing costs limit GaAs technologies such as III (Al, Ga, In) - V (N, P, As, Sb) multi-junction solar cells despite achieving maximum efficiencies of 44.7% (Dimroth et al. 2014; Jean et al. 2015). Thin films, on the other hand, are constructed of thin semiconductor layers with a solid backing material which reduces the quantity of material required and therefore the production cost compared with regular Si cells (Lechner and Schade 2002; Parida et al. 2011).

Thin-film types include a-Si the most commercial film due to its abundance and non-toxicity with flexible module production and low substrate cost, giving efficiencies of 5%–7% but is susceptible to degradation (Chopra et al. 2004; Parida et al. 2011). Cadmium telluride (CdTe) is a stable compound with a direct bandgap and large absorption coefficient producing cell efficiencies of 21 % (First Solar Press Release 2014) that can be synthesized via a wide variety of methods although showing high parameter variation in identical devices (Jäger-Waldau 2004; Lee and Ebong 2017).

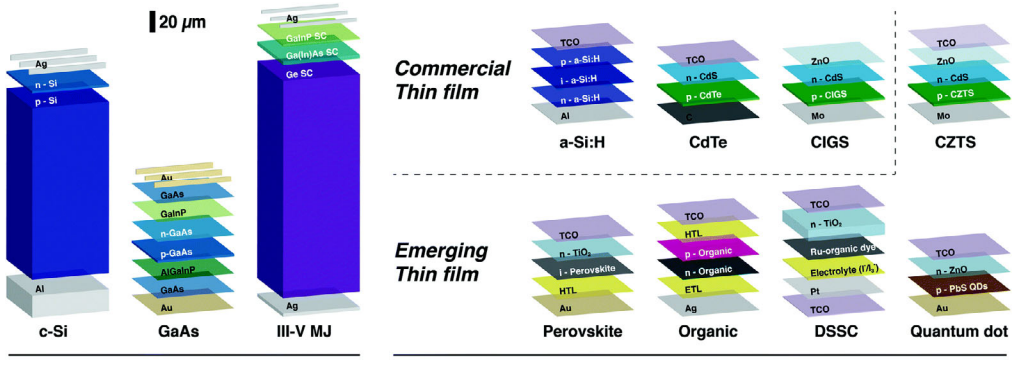

Fig. 1 PV technologies suitable for window integration. Wafers c-Si, GaAs, III-V and thin films (Jean et al. 2015; reprinted with permission ©2015 Royal Society of Chemistry)

Copper indium gallium diselenide (CIGS) shows maximum efficiency of 22.3% manufactured in lightweight building material products with further research currently investigating its use in flexible substrates for better efficiencies at low-cost and longer-lasting devices (Green et al. 2017; Haegel et al. 2017). Emerging thin-film technologies include Cu_2ZnSnS_4 (CZTS), similar to CIGS, although with non-abundant element where Zn and Ga replaced In and Sn, respectively (Polman et al. 2016), with the highest efficiencies at 12.6% (Wang et al. 2014b). Nevertheless, there are voltage losses observed in CZTS due to recombination at bulk material defects and charge extraction interfaces. Perovskite is a low cost manufacturing compound made from hybrid organic-inorganic lead or tin halide-based material with a light-harvesting active layer, with a 22.7% record high efficiency (Manser et al. 2016; Hamers 2017; National Renewable Energy Laboratory 2017). On the other hand, organic photovoltaics (OPVs) that use organic compounds (typically made of polymer and small molecules) as semiconducting materials instead of silicon have excellent prospects. These organic semiconductors combine cheap production cost and plastic properties and can be processed by techniques not available to crystalline silicon semiconductors, unfortunately, their power conversion efficiencies are low within the range of 3%–11% (Spanggaard and Krebs 2004; Krebs 2009; Hoppe and Sariciftci 2004; Green et al. 2015). Dye-sensitized solar cells (DSSC) are comprised of TiO_2, a dye, an electrolyte and a conductive glass. The working principle of DSSC starts with incident light upon the surface of the solar cell being absorbed by the dye molecules causing electron excitation. Electrons in the excited state of the dye are then transferred to the back contact with electrons then flowing through an external circuit to provide electrical charge. Electrolytes can be used as an electron mediator between the TiO_2 and counter electrode (Chang et al. 2013; Skandalos and Karamanis 2015). Quantum dots (QDs), are semiconductor nanocrystals that have diameters of less than 10 nm and due to their size-dependent photoluminescence, chemical stability, broad excitation range, narrow emission peak and tunable stocks shift and degradation resistance compared with traditional organic dyes they became a promising material for several research fields (Zheng et al. 2019).

Conventional Si PV cells are now a well-established technology with an emerging trend in using them as semi-transparent PV (STPV) replacing glazing in buildings. This technology consists of common solar cells encapsulated between glass panes using EVA (ethylene vinyl acetate) film with variations of glazing transparency achieved via separation of the PV cells at different distance intervals (Skandalos and Karamanis 2015). Thin PV films have gained a lot of attention due to their low cost and high optical absorbance, combining the energy-producing with the high transparency when comparing against Si cells, thus being suitable for building integration to get better indoor conditions, although with lower efficiencies limiting to expand their usage (Lechner and Schade 2002). Table 1 shows examples of building integration, efficiencies and transmittance for Si mono- and poly-crystalline, amorphous Si, thin films (CIGS and CdTe), organic PV and DSSC.

2.2 PV windows

Semi-transparent PV windows are an effective solution for simultaneously providing electricity generation and daylighting with various degrees of solar heat and natural light penetration (Wah et al. 2005). However, it is important to ensure that these PV windows have good electrical performance as well as suitable transparency levels and colours to satisfy visual needs and comfort. Hence, the two main goals for PV window performance optimization are improving daylighting and energy production (Hee et al. 2015). In addition, the interaction between PV windows and buildings cannot be neglected. There is a variety of simulation tools available for predicting the performance of PV windows and their effects on building performance in the aspects of indoor

Table 1 Integration of crystalline and amorphous Si solar cells, CIGS solar cells, CdTe solar cells and Dye-sensitised solar cells into buildings as part of façade, window, cladding panels and roof

PV technology	Building integration	Efficiency	Transmittance
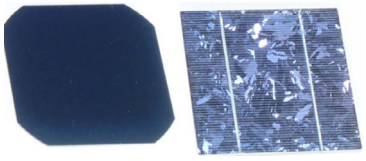 Mono c-Si solar cell (left) Poly c-Si solar cell (right) (Ogbomo et al. 2017; reprinted with permission ©2017 Elsevier)	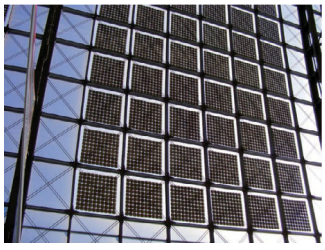 c-Si PV façade (Heinstein et al. 2013)	14%–22% (Jelle and Breivik 2012)	May vary as the gap among cells
 a-Si solar cell (Skandalos and Karamanis 2016; reprinted with permission ©2016 Elsevier)	 a-Si PV window (Skandalos and Karamanis 2016; reprinted with permission ©2016 Elsevier)	5%–10% (Parida et al. 2011)	8% (Leite Didoné and Wagner 2013)
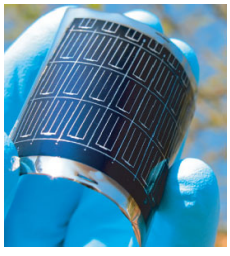  CIGS solar cell (left) (Ramanujam et al. 2020; reprinted with permission ©2020 Elsevier) CdTe solar cell (right) (Alrashidi et al. 2019; reprinted with permission ©2019 Elsevier)	 CdTe PV window (Sun et al. 2018; reprinted with permission ©2018 Elsevier)	16% (Kessler et al. 2003), 9% (Ullal et al. 1997)	Up to 85% (Khairnar et al. 2003)
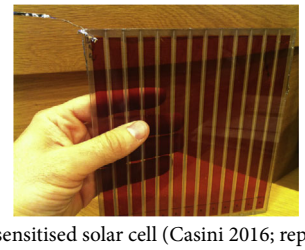 Dye-sensitised solar cell (Casini 2016; reprinted with permission ©2016 Elsevier)	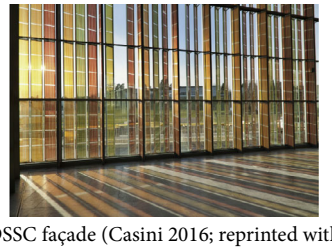 DSSC façade (Casini 2016; reprinted with permission ©2016 Elsevier)	10% (Kroon et al. 2007), 6% (Späth et al. 2003)	30% (Leite Didoné and Wagner 2013), 60% (Kang et al. 2003)

comfort, onsite electricity generation and energy demands for heating, cooling and artificial lighting. Such tools include Daysim, EnergyPlus, Ecotect, DesignBuilder, ESP-r, PVsyst, COMFEN, PROMETHEE and StatSoft. For the design of PV windows, various parameters need to considered, such as window to wall ratio (WWR), orientation, transmittance and power conversion efficiency, since each plays an important role in window performance and will therefore have repercussions for building performance.

A global feasibility evaluation for DSSC based STPVs was investigated by Lee et al. (2014) in 6 representative cities with diverse climate zones: Miami (zone 1), Sao Paulo (zone 2), Sydney (zone 3), New York (zone 4), Seoul (zone 4), Berlin (zone 5) and Moscow (zone 6). Energy simulation was conducted via ESP-r with the model constructed in accordance with standard building envelope parameters from the American Society of Heating, Refrigerating and Air-Conditioning Engineers (ASHRAE). The results showed

that the percentages of the total building energy consumption offset by the electricity generation from the STPVs were 12% for Miami, 20.5% for Sao Paulo, 18.9% for Sydney, 21.9% for New York and 15.9% for Seoul, indicating the suitability of the STPVs in zones 1 to 4 (hot to mixed climates). For cold climatic zones Berlin and Moscow, the benefits of using the STPVs for improving building energy efficiency were not significant. The study also revealed that the STPV window can be optimized in terms of WWR, orientation and visible transmittance to achieve better energy performance of buildings.

Wong et al. (2008) evaluated the application of polycrystalline silicon-based STPVs in different climatic regions in Japan and highlighted the influence of glazing optical properties on building performance. The thermal balance, power generation, daylighting and indoor conditions in a house with a south-facing BIPV roof were modelled and validated against experimental results. The results showed that applying a BIPV roof consisting of an STPV top light with a radiance transmission of 50% can achieve annual energy savings of 3.0% in Kagoshima (warm region) and 8.7% in Aomori (cold Region), as compared with a completely opaque BIPV roof. In contrast, applying a BIPV roof consisting of an STPV top light with a radiance transmission of 20% had a negligible energy-saving effect due to lower solar heat gains and thus lower benefits in heating energy savings.

Chae et al. (2014) prepared three different semi-transparent solar cells: an untextured solar cell with a 120-nm-thick a-Si:H absorber (PV1), an untextured solar cell with a 180-nm-thick a-Si:H absorber (PV2), and a textured solar cell with a 180-nm a-Si:H absorber (PV3) for integration within double glazing. The double glazing with PV1 had both the highest visible transmittance (VT) and solar heat gain coefficient (SHGC), while the one with PV3 exhibited both the lowest VT and SHGC but the highest power conversion efficiency. EnergyPlus simulations were conducted to compare the performance of the STPV systems in six American cities: Miami, Phoenix, Los Angeles, Baltimore, Chicago and Duluth. The results showed that the double glazing with PV 3 offered the highest annual electricity generation in all the selected cities. In terms of saving energy, it is hard to determine which STPV system is the best. For example, using the double glazing with PV3 contributed to the lowest HVAC energy usage in the low-latitude cities (e.g., Miami), but the highest HVAC energy usage in the high-latitude cities (e.g., Duluth). Concluded from the studies of Wong et al. (2008), Chae et al. (2014), and Lee et al. (2014), careful selection of STPV types with suitable thermo-optical characteristics in different climatic regions is important for the energy efficiency of buildings.

Chen et al. (2012) characterised different types of thin-film STPV glazing units under varying environmental conditions using an indoor calorimetric hot box and solar simulator developed by the Solar Energy Research Institute of Singapore (SERIS). The findings showed that the SHGCs and electric power outputs of the STPVs changed significantly when the angle of incident solar radiation was greater than 45 °C. This study provides a method to obtain the angular dependent SHGCs and electrical parameters of STPVs which can serve as inputs to PV thermal and electrical models for building performance simulation.

Ng et al. (2013) investigated the performance of various commercially available windows in the climate of Singapore by EnergyPlus simulation with the input data of windows' SHGCs and *U*-values from measurements. A comparative analysis was conducted among three amorphous silicon (a-Si) based STPVs, three micromorph silicon (μc-Si) based STPVs and four conventional windows over different WWRs varied from 70% to 100%. The results showed that all the STPV windows under investigation contributed to less annual total electricity consumption compared with the conventional windows, and larger energy savings were achieved with the increase of WWR.

Similar findings regarding the effect of WWR were observed in the studies (Liao and Xu 2015; Sun et al. 2018; Chen et al. 2019). Liao and Xu (2015) explored the relationship between the performance of a-Si based STPVs and the architectural conditions including WWR, window height and room dimensions. The simulation results indicated that using a-Si based STPVs is more beneficial in saving energy than conventional glazings for shallow rooms with large WWRs. Chen et al. (2019) evaluated the potential application of c-Si based PV windows under various climatic conditions in southwest China. A comprehensive simulation approach that combined a heat transfer model, daylighting model and Sandia PV model in EnergyPlus, was developed and validated against field measurement results. The annual total energy consumption of the test room in the climate of Chengdu was predicted to reduce from 1178 kWh to 648 kWh when the WWR was increased from 8% to 83%, due to the increased electricity output as a result of the increased PV cell area.

In contrast with see-through a-Si PV cells, the integration of opaque c-Si PV cells in glass envelopes can cast shadows in the building interior and limit the viewing from inside out (Skandalos and Karamanis 2015). To deal with this problem, Peng et al. (2019) introduced a novel BIPV insulated glass unit (BIPV IGU) based on a c-Si cell in narrow strips. Compared with traditional c-Si based PV glazings, the BIPV IGU has the advantage of providing a more uniform light distribution in the building space (see Figure 2) without compromising power conversion efficiency. The BIPV IGU was characterised by outdoor experiments at the Lawrence Berkeley National Laboratory (LBNL). During a test period

Fig. 2 (a) External view and (b) internal view of the BIPV IGU consisting of narrow c-Si cell strips (Peng et al. 2019; reprinted with permission ©2019 Elsevier)

of two months (from October 1st to November 30th, 2015), the electricity output from the BIPV IGUs with overall dimensions of 5.9 m × 1.8 m was measured to be 1940 Wh/day, which can fully cover the artificial lighting electricity usage of the test room, 431 Wh/day.

Apart from saving energy, the use of semi-transparent PVs can reduce the risk of visual discomfort caused by excessive daylighting or glare in buildings (Sun et al. 2018). Sun et al. (2018) assessed the annual daylight performance of a side-lit cellular office where the window was partially covered by cadmium telluride (CdTe) PV glazing. The useful daylight illumination (UDI) and daylight glare probability (GDP) metrics were applied to evaluate the daylight availability and glare discomfort within the office space, respectively. RADIANCE simulations conducted under the Harbin and Guangzhou climates in China showed that working hours percentage with desired illumination levels (i.e., 100 lux ≤ UDI ≤ 2000 lux) and imperceptible glare (DGP ≤ 0.35) were improved when increasing the PV glazing coverage ratio. Cannavale et al. (2017) explored the potential of a perovskite-based PV window in glare protection for an office-type environment. The results from daylight simulation via Daysim showed that in the climate of London, the occurrence of high DGP (> 0.45) was reduced from 49% (for a clear glass window) to 16% by applying the PV window. In the study by Liu et al. (2020), the performance of CdTe based PV windows with varying degrees of visible transmission and WWRs was simulated using RADIANCE, and comprehensively evaluated in terms of daylight availability, daylight distribution, glare discomfort and colour quality. Complementary to the above findings, in Table 2 can be seen a summary of relevant simulation work conducted on building integrated semi-transparent PVs.

2.3 PV shading devices

In addition to the use of BIPV as windows, BIPV can also be used as window associated components such as shading devices, exterior cladding panels, etc., which can provide control of solar heat and daylight into buildings and meanwhile generate energy onsite (Peng et al. 2011; Jelle et al. 2012b; Delisle and Kummert 2014; Youssef et al. 2018). Figure 3 shows examples of BIPV integrated as shading devices. Radut and Mihai (2015) developed a multifunctional integrated photovoltaic window (MIPVW) consisting of photovoltaic blinds with advanced maximum power point tracking (MPPT) powered by a stepper motor. The results showed that compared with a PV window with similar characteristics, the MIPVW generated 20% more energy. Kang et al. (2012) assessed the performance of a double-skin façade (DSF) integrated with PV attached venetian blinds. Numerical models were developed for the DSF with PV blinds, followed by a parametric analysis concerning the PV blinds' tilt angle, azimuth, length, width and distance from the outer glass pane. It was found that changing the width and tilt angle of the PV blinds can pose a significant influence on the shading phenomena and energy generation. Additionally, when the DSF was unventilated, the maximum temperature of the PV blinds reached 78 °C and the power conversion efficiency reduced from 14.1% (at 25 °C) to 10.4%; while when ventilated, the maximum temperature was 58.4 °C and the PV blinds had a greater efficiency of 11.7%. The energy produced was 509 Wh/m^2 in the daytime. Kim et al. (2010) developed a shading device composed of multiple louvres coated with PV cells for building application. The slat angle of the louvres was adjustable by using a computer-controlled motor according to measured climatic conditions. The results showed that the energy generated and daylight intensity in the interior space were both largely dependent on the slat angle. Sun and Yang (2010) studied the tilt-angle impact of shading-type BIPV claddings on the energy performance of a building in Hong Kong and found that 20° is the optimum tilt angle for maximum electricity generation. When taking both electricity generation and cooling load reduction into account, the optimum tilt angle varied between 30° and 50°, depending on the cladding

Table 2 Summary of relevant simulations performed on STPV featuring characteristics of STPV as WWR transmittance, efficiency and software used

Type	Building components	Simulation tools	WWR	Transmittance	Efficiency	Ref.
Organic, a-Si	STPV window	EnergyPlus	<50%, >50%	30%, 8%	3%, 5%	Leite Didoné and Wagner 2013
Poly-Si	STPV roof	EnergyPlus	—	20%, 50%	14.3%	Wong et al. 2008
a-si,μc-Si	STPV windows	EnergyPlus	10%–100%	50%, 80%	8%, 5.9%, 3.3%, 4.4%, 5%, 4.7%	Ng et al. 2013
a-Si, mono-Si, CuInSe	STPVs	—	—	20%	6%, 17%, 11%	López and Sangiorgi 2014
Si	STPV window	EnergyPlus	20%–70%	—	—	Xu et al. 2014
Si	Semi-transparent single-glazed	EnergyPlus	—	20%	—	Lu and Law 2013
a-Si	Double glazed module	TRNSYS	—	10%	7%	Song et al. 2008
Poly-Si, a-Si, Organic	STPV window	Daysim, EnergyPlus	40%, 60%	10%–50%	15%, 10%	Kapsis and Athienitis 2015
DSSC, Multi-Si, a-Si	Window	Ecotect	50%	25%, 30%, 38%, 45%	7%	Yoon et al. 2011b
	Skylight	—	—	20.1%	10.8%	Li et al. 2009b
	STPV windows	DesignBuilder, EnergyPlus, PVsyst, and COMFEN	11%–88%	10%, 20%, 30%, 40%	—	Olivieri et al. 2014
Mono-Si	South-facing shading PV device	PROMETHEE	—	—	—	Stamatakis et al. 2016
Poly-Si	STPV glazing module	—	—	92%, 43%	—	Park et al. 2010
a-Si, μc-Si	STPV windows	EnergyPlus	43%	10.6%	6.3%	Li et al. 2009a
a-Si	STPV window	StatSoft	—	10%	7%	Yoon et al. 2011a

(a) (b)

Fig. 3 Different PV shading devices, (a) with a more aesthetical approach (Jayathissa et al. 2017; reprinted with permission ©2017 Elsevier) and (b) with louvers design (Kang et al. 2012; reprinted with permission ©2012 Elsevier)

heights. Yoo and Lee (2002) assessed the electrical performance of BIPV modules when installed as sunshade panels on the façade and roof of a commercial building in R.O. Korea. Using one year of analysis, the average power conversion efficiency of the sunshade panels on the south façade was 9.2%, with a maximum of 20.2% in winter and a minimum of 3.6% in summer.

2.4 PV-thermal (PV/T) collectors

Combining PV and thermal collector (PV/T) technologies have gained significant attention since they solve the issue of undesired overheating of solar cells (Michael et al. 2015; Sahota and Tiwari 2017) which causes decreased efficiency by an increase in resistance. PV/T systems are engineered to carry heat away from the PV cells thereby cooling the cells and improving their efficiency by lowering resistance (Da Silva and Fernandes 2010; Buker and Riffat 2015; Lämmle et al. 2017). Solar collectors are divided into two groups: non-concentrating (stationary) and concentrating (dynamic). Stationary collectors have flat surfaces to absorb solar rays, whilst concentrating collectors have concave

reflecting surfaces to focus solar rays into a smaller receiving area (Kalogirou 2004; Tyagi et al. 2012). Figure 4 shows schematics of a stationary collector and a parabolic-trough collector with a tracking system.

PV/T collector technologies can be developed by combing crystalline or amorphous silicon PV, liquid or air collectors, a flat plate or solar concentrating device with or without a transparent cover (Hansen et al. 2018). Additionally, the absorber structure changes according to the needs of the system, i.e., flat plate tube, extruded heat exchanger, rectangular tunnel with or without fins, sheet-and-tube structure, roll-bond heat exchanger and micro-channel heat pipe array/heat mat (Wu et al. 2017). The electrical efficiency of a PV/T module can be calculated based on a measured I-V curve with Eq. (1), and the thermal efficiency can be calculated by Eq. (2) (Chow 2010).

$$\eta_e = \frac{V_{mpp} I_{mpp}}{GA} \tag{1}$$

$$\eta_t = \frac{\dot{m} C (T_{out} - T_{in})}{GA} \tag{2}$$

where $\dot{m}$ is the mass flow rate; C the specific heat capacity of the coolant; T_{in} and T_{out} are the coolant temperatures at the inlet and outlet, respectively; A is the collector aperture area; G is the incident solar irradiance normal to surface; V_{mpp} and I_{mpp} are the voltage and current at maximum power point operation, respectively.

Davidsson et al. (2010) developed and modelled a hybrid solar window composed of PV cells (for electricity generation), water pipes (for thermal energy collection) and tiltable reflectors (for solar concentration and daylighting control). Basically, the incoming radiation was either focused onto the PV cells or transmitted into the indoor space when the reflectors operated in a closed or open mode, respectively, which controlled the daylight amount entering the building. Meanwhile, high PV efficiencies were maintained by active water cooling on the backside of the PV cells, and the hot water was delivered for domestic use. The simulation results showed that the electricity generation can be increased by 35% using this prototype as compared with flat PV modules. In another project by Davidsson et al. (2012), the previous designed solar window was connected to a thermal storage tank of 620 L, as shown in Figure 5, and the intricate relation between the PV/T window and the building was investigated. The findings showed that the auxiliary energy load of the building was 1000 kWh less using an individual solar collector and PV

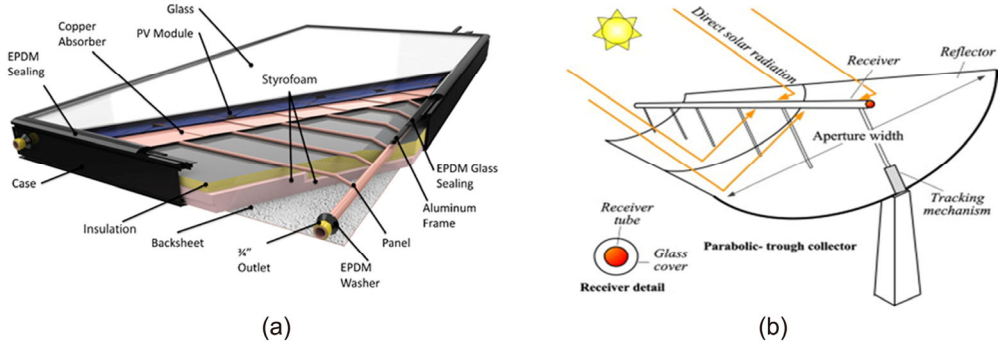

Fig. 4 (a) Components comprising a stationary PV/T (Michael et al. 2015; reprinted with permission ©2015 Elsevier) and (b) schematic design of a parabolic-trough collector with tracking system (Cabrera et al. 2013; reprinted with permission ©2013 Elsevier)

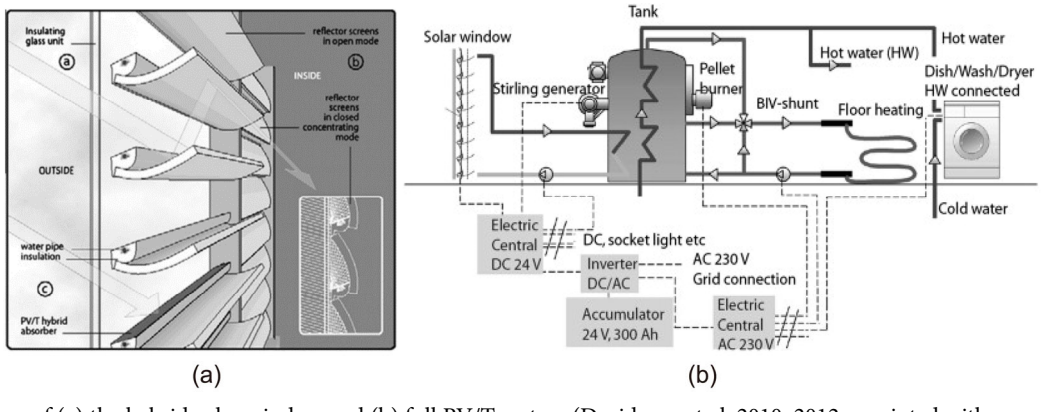

Fig. 5 Depiction of (a) the hybrid solar window and (b) full PV/T system (Davidsson et al. 2010, 2012; reprinted with permission © 2010, 2012 Elsevier)

modules on the roof compared against using the PV/T window. If the solar collector was removed from the building, the auxiliary energy load was around 600 kWh larger than that when the PV/T window was used.

Ulavi et al. (2014) presented a PT/V window integrated with compound parabolic concentrators (CPCs) coated with a wavelength selective film, which allowed the visible portion of the sunlight to enter buildings for illumination and concentrated the infrared portion onto the PV/T absorber for electricity generation and hot water production. The optical performance of the PV/T device in vertical and horizontal positions as a window and skylight respectively was analysed by Monte-Carlo ray-tracing simulations. The thermal efficiency has ranged from 18% to 24% for the south-facing window with CPC geometries ranging $-25° \leq$ Nominal half-acceptance angle (θ_c) $\leq 45°$.

Sabry et al. (2014) developed a CFD model to predict the performance of a double-pane window integrated with PV/T solar collectors, which consisted of water-cooled GaAsP/InGaAs quantum well square (QWSC) solar cells with a power conversion efficiency of ~32% and two-axis tracking solar concentrators with a concentration ratio of 500×. It was found that the temperature of the water passing through the PV/T solar collectors was increased by 5 K, under an incident solar radiation of 800 W/m^2, an ambient temperature of 273 K, a water inlet temperature of 283 K and a water flow rate of 0.01 kg/s.

2.5 Summary of BIPV glazing system studies

This section highlights the features of existing BIPV glazing technologies and summarises the main findings from relevant studies. By far, a variety of solar cells, such as silicon, CdTe, Perovskite, organic and dye-sensitised solar cells, have been developed and integrated into building envelope components such as window, skylight, double-skin façade and shading device (see Table 3). Window integrated crystalline silicon (c-Si) PV is a well-established technology with high power conversion efficiency, however, may not be suited to building areas where uniform daylight distributions and unobstructed views of the external environment are required. Thin-film PVs such as amorphous silicon (a-Si) solar cells show advantages over c-Si PVs in terms of visual and aesthetic aspects but can be inferior in electricity generation. To achieve a good visual effect without compromising the power conversion efficiency, a promising approach is to cut standard high-efficiency c-Si PV cells into narrow strips and laminate them with glasses.

In the past decades, extensive research has been conducted to investigate the characteristics of different types of semi-transparent PVs (STPVs) and their effects on building energy and daylight performance. A common finding is that using STPVs can contribute to lower solar heat gains and cooling loads of buildings compared with conventional clear or Low-e glazings, but also offset a proportion of electricity consumption by on-site power generation. However, the use of STPVs can potentially increase the heating and artificial lighting loads of buildings. Although a large body of research has shown that using STPVs can effectively reduce the annual total energy consumption of buildings, most of the tests were conducted in hot or cooling-dominated climates. The energy savings in cold climates by using STPVs were generally minor or negligible. Moreover, the extent of energy-saving is largely dependent on the WWR, orientation and thermo-optical characteristics of STPVs. Apart from saving energy, STPVs have been proved to be effective in reducing the occurrence of excessive daylighting and glare in buildings, thereby improving the visual comfort of occupants. PV/T window which combines PV cells, solar thermal collectors and solar concentrators (optional) in a glazing unit is another promising technology for generating electricity while producing hot water for indoor usage.

Table 3 Summary of materials, applications, technologies and benefits of BIPV

BIPV	PV type	Application	Energy saving & generation	Benefits
PV window/façade	Thin films multi-junction, organic PV cell, DSSC	Office, residential, windows, façades	Energy generated comprised 12%–20% of building consumption in 5 different locations (Lee et al. 2014), can save 30% of the total HVAC system energy comparing against double-pane glass (Chae et al. 2014)	Thermal balance, daylight and indoor controlled conditions
Shading/cladding PV/roof	c-Si, wafer, thin film, organic	Venetian blind, louvers, cladding, sun-shade PV modules, roof-mounted PV modules	20% more energy generation than vertical glazing PV window (Radut and Mihai 2015), power generation can achieve 509 Wh/m^2 (Kang et al. 2012)	Daylight, environment and indoor overheating protection
PV/thermal	c-Si, GaAsp/InGaAs	PV sunshade module and thermal collector	35% more energy production per unit area of PV cells against flat PV module on vertical position (Davidsson et al. 2010)	Overheating, daylight control, boiling water

3 Building integrated concentrating PV (BICPV) systems

Concentrating photovoltaic (CPV) is a combination of PV cells or modules with an optical system. This optical system or so-called solar concentrator is used to increase solar flux hitting the PV area, working at higher irradiation levels than conventional PV arrays and obtaining a higher conversion efficiency (Algora and Rey-Stolle 2016; Lamnatou and Chemisana 2017). CPVs can be classified into four types according to geometric concentration ratio C_g (i.e., the ratio of the concentrator aperture area to the PV aperture area): low concentration PV systems (C_g < 10×), medium concentration PV systems (C_g = 10–100×), high concentration PV systems (C_g = 100–200×) and ultra-high concentration PV systems (C_g > 2000×) (Shanks et al. 2016). High CPV systems require mechanical tracking systems with low tolerances of usually less than 0.2° and need more space for installation making building integration more complex. Medium CPV systems also require tracking systems; however, by decreasing the geometric concentration ratios building integration can be achieved. Conversely, low CPV systems (C_g < 4×) do not depend on solar tracking as they are based on non-imaging optics with wide half-acceptance angles (i.e., the angle of incident radiation on a solar concentrator when 90% of the maximum power is generated), allowing the collection of both direct and diffuse radiation (Sarmah et al. 2011; Li et al. 2013; Baig et al. 2014b). Hence low CPV systems can remain static, therefore suitable for façade and window applications (Sarmah et al. 2011; Li et al. 2013; Baig et al. 2014b).

3.1 Parabolic concentrator based CPV glazing systems

The integration of a PV system into a window requires analysis of which technology will best suit the building needs, given that every scenario and location is different (Shanks et al. 2016). Once difficulties such as concentrator geometry design and elimination of tracking systems are resolved CPV windows are an excellent option to produce clean onsite energy (Sellami and Mallick 2013). In addition, CPV can also be used as shading devices, therefore offering several integration ways to reduce energy consumption in buildings. Technologies such as compound parabolic concentrators (CPC) and V-trough reflectors show good potential for building integration due to their effective solar concentration performance and lower PV cell usage compared with regular PV panels (Singh et al. 2016). Novel designs of 2D and 3D CPC are acknowledged as one of the best stationary designs. Figure 6 shows the variant designs of CPCs. Relevant work performed on CPV systems for building integration are summarized in Table 4.

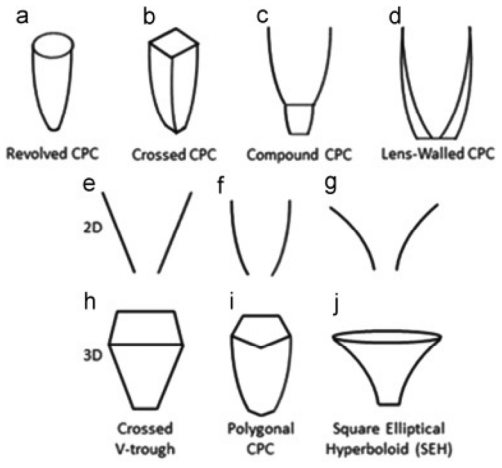

Fig. 6 (a) The revolved CPC; (b) the crossed CPC; (c) the compound CPC; (d) the lens-walled CPC; (e) V-trough; (f) CPC; (g) compound hyperbolic concentrator; (h) 3D square aperture V-trough; (i) polygonal aperture CPC; (j) hyperboloid with an elliptical entry aperture and square exit aperture (Shanks et al. 2016)

Abu-Bakaret al. (2015b) assessed the performance of a low CPV system with a geometrical concentration ratio of 3.6×, which consisted of a 1 cm × 1 cm monocrystalline laser grooved buried contact Si solar cell and a rotationally asymmetrical compound parabolic concentrator (RACPC). The RACPC had an optical efficiency of 84% at a normal incidence and a half-acceptance angle of 43°. The I-V characteristics of the CPV system were measured at the standard test conditions (AM1.5, 1000 W/m^2 and 25 °C cell temperature), showing that the RACPC increased the maximum power output of the system by up to 3.33× in comparison to a non-concentrating cell.

The outdoor characterisation of a 300 mm × 300 mm CPV module was presented by Sarmah and Mallick (2015), which consisted of Dielectric Compound Parabolic Concentrators (DiACPCs) with two strings of 14 solar cells connected in series. The DiACPC module had a geometric concentration ratio of 2.8× and half-acceptance angles of 0° & 55°. The CPV module and a similar non-concentrating system were tested in Edinburgh in different weather conditions. The results showed that the DiACPC module had average maximum power outputs of 0.13 W and 5.88 W during the tested rainy and sunny days, respectively, being 2.17 and 2.27 times higher than those of the counterpart system, respectively.

Bunthof et al. (2016) investigated the impact of shading on three CPV systems by outdoor experiments. The first system comprised of a 10 cm × 10 cm PMMA-Fresnel lens-based concentrator with a 1 cm × 1 cm TJ cell placed on the lens' focal point. The second system consisted of a 4 cm × 4 cm planar focusing optic with a 1.3 mm × 1.3 mm TJ III/V cell, a bypass diode, a copper heat sink and

Table 4 CPV window integration featuring concentrator type, acceptance angles and concentration ratio

Types	Prototypes	Concentration ratios	Building integration	Acceptance angles	Ref.
3D static square elliptical hyperboloid	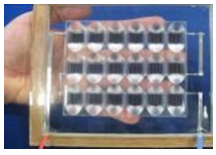	4×	Windows pane/glass	120° (−60°, +60°)	Sellami et al. 2012; reprinted with permission ©2012 Elsevier
Linear asymmetric compound parabolic concentrator	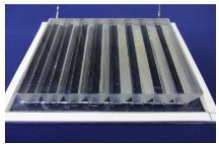	2.8×	Windows	0–55°	Baig et al. 2014a; reprinted with permission ©2014 Elsevier
Three-dimensional cross geometric compound concentrator	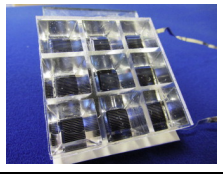	3.6×	Windows pane/glass	70°	Baig et al. 2014b; reprinted with permission ©2014 Elsevier
Truncated dielectric asymmetric compound parabolic concentrator	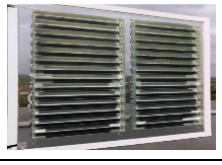	2.8×	Windows	0–55°	Baig et al. 2016; reprinted with permission ©2016 Elsevier
RADTIRC (rotationally asymmetrical dielectric totally internally reflecting concentrator)		4.9×	Double glazing window	±40° along the *x*-axis and ±30° along the *z*-axis	Abu-Bakar et al. 2016; reprinted with permission ©2016 Elsevier
RACPC (rotationally asymmetrical compound parabolic concentrator)	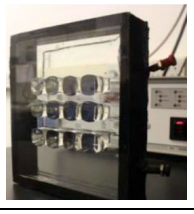	3.66×	Double-glazing window	0–60°	Ramirez-Iniguez et al. 2017; reprinted with permission ©2017 Elsevier
PRIDE (photovoltaic façades of reduced costs incorporating devices with optically concentrating elements)	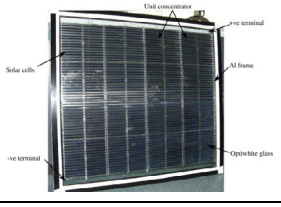	2.45×	building façade integration	0–66°	Mallick and Eames 2007; reprinted with permission ©2007 Elsevier
DiACPC (concentrating dielectric compound parabolic concentrator)		2.8×	building façade integration	Half angles of 0° & 55°	Sarmah and Mallick 2015; reprinted with permission ©2015 Elsevier

integrated wiring. The third system was a 4 × 4 array of the proposed planar focusing optics with integrated solar cells. Similar concentration efficiencies were observed for the Fresnel lens-based system and single planar optic based system, which were 0.62 and 0.66–0.77, respectively, indicating similar solar concentration performance. However, the Fresnel lens system needs a large air cavity to account for optical focal depth, while the planar optic based system has

no such requirement and is more suitable for integration into building envelope components such as windows. Moreover, this research showed that the multi-planar-optics system suffered a loss in performance from 7% to 12% under shading, and it was recommended to reduce the number of series interconnections among solar cells in the system for building areas where system shading commonly occurs.

Fernández et al. (2014) proposed an artificial neural network model to calculate the maximum power output of low CPV modules, using direct irradiance, diffuse irradiance, module temperature and solar incidence angles. The findings demonstrated that the model could estimate the maximum power output of a low CPV module for building integration with a margin of error: R^2 = 0.99, MBE = −0.05% and RMSE = 2.32%, and can give accurate predictions on both clear days and cloudy days.

3.2 Luminescent solar concentrator based CPV glazing systems

In the 1970s and 1980s, special attention was given to fluorescent concentrators (Weber and Lambe 1976; Goetzberger and Greube 1977) with luminescent solar concentrators (LSC) gaining consideration as a PV substitute due to their lower cost and the ability to harness direct and diffuse solar rays, therefore avoiding expensive tracking systems (van Sark 2013). LSC can be seen as a matrix of dye molecules that absorb light and then re-emit it at longer wavelengths, thus light is internally reflected via total internal reflection (TIR) and guided to the edges where solar cells are placed (Chemisana 2011). Figure 7 and Figure 8 show how an LSC works (Goldschmidt 2012) and samples of LSC in different colours under UV light, respectively. Also, LSCs can provide architectural features for being lightweight, coming in various colours and degrees of transparency, and for being flexible which made them a versatile product for incorporation into buildings. For example, they are particularly suitable for either windows panes or glazed façades. Despite

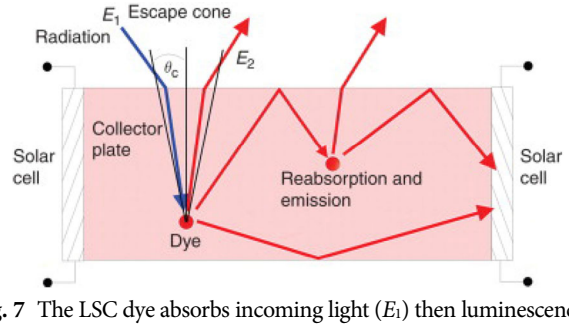

Fig. 7 The LSC dye absorbs incoming light (E_1) then luminescence is randomly emitted (E_2). The photons re-emitted at angles within the escape cone leave the LSC, and the rest photons are guided to the LSC's edges by total internal reflection (Goldschmidt 2012; reprinted with permission ©2012 Elsevier)

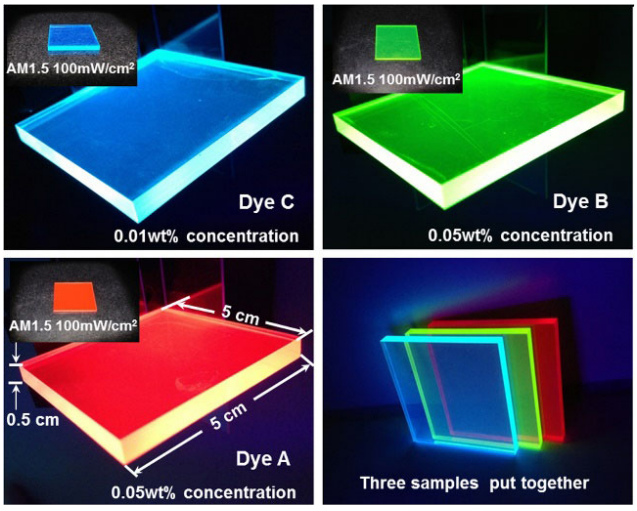

Fig. 8 Three LSC samples of 5 cm × 5 cm × 0.5 cm size; Dye C LSC with 0.01 wt.% concentration, Dye B with 0.05 wt.% concentration, Dye A with 0.05 wt.% concentration representing blue, green and red colour respectively under UV light (Liu and Li 2015; reprinted with permission ©2015 Elsevier)

the ability of LSC to collect both direct and diffuse radiation potential downsides relate to the colouring, directly related to the dyes and subsequent energy efficiency, affecting indoor visual comfort and lighting needs (Aste et al. 2017). LSC efficiency is related to the overall absorption of the dyes, fluorescence & trap efficiency, refractive index of the plate and stoke efficiency and due to these factors LSC efficiency is currently around 7%. Future research is needed to solve the drawbacks like self-absorption of the luminescent dyes and escaping emissions beyond the critical angle (Reisfeld 2010).

It should be noticed that LCSs are commonly manufactured by doping organic dye or Quantum dots (QD) into a transparent plastic sheet (Currie et al. 2008). Organic dyes are π–conjugated organic molecules, where the core is flat with all atoms of the conjugated chain lying on the same plane linked by σ-bonds. Absorption bands are the promotion of π–electrons above and below this plane along the conjugated chain moving from a ground energy state to an excited higher energy state (van Sark et al. 2008). Organic dyes can provide high luminescence quantum efficiency (LQE) (near unity), a wide range of colours and improved re-absorption properties with UV stability in new molecular species. Table 5 summarizes commercial dyes describing absorption, emission and quantum yield (Slooff et al. 2006; van Sark et al. 2008).

As compared with organic dyes, quantum dot crystalline semiconductors feature less degradation (Chemisana 2011), permitting to control of the red shift between absorption and luminescence and reducing re-absorption yielding better efficiencies and concentration ratios via dot's sizes

Table 5 A summary of commercial dye characteristics including absorption, emission and quantum yield

Dye	Absorption λ_{max} (nm)	Emission λ_{max} (nm)	Quantum yield (%)
Lumogen F Blue 650	377	411	>80
Lumogen F Violet 570	378	413	94
Lumogen F Yellow 083	476	490	91
Lumogen F Yellow 170	505	528	>90
Lumogen F Orange 240	524	539	99
Lumogen F Red 305	578	613	98
Red G	520	600	87
CRS040 (CFS002 Yellow)	440	506	98

(Barnham et al. 2000). An important aspect of quantum dots is the quantum yield, described as the quantity of fluorescing photons to the materials incident photons (Norton et al. 2011). Moreover, QDs have different emission colours directly proportional to their size. Figure 9 (Bera et al. 2010) illustrates the variation of photoluminescence emission colour with size for CdSe QD. Additionally, QDs stand out for having a large range of applications from bio-imaging, nanomedicine, PV cells, organic polymers, OLED technology and more (Kamat 2013; Jin et al. 2015; Stanisavljevic et al. 2015; Bak et al. 2016; Bonilla et al. 2016; Dayneko et al. 2016; Dovzhenko et al. 2016; Finetti et al. 2016; Linkov et al. 2016; Shen and Liu 2016; Sukhanova et al. 2016; Tabish and Zhang 2016; Tavakoli 2016; Volkov 2015). Complementary information about the features, doping methods, relevant research and applications of quantum dots can be found in the review paper of Wei et al. (2019).

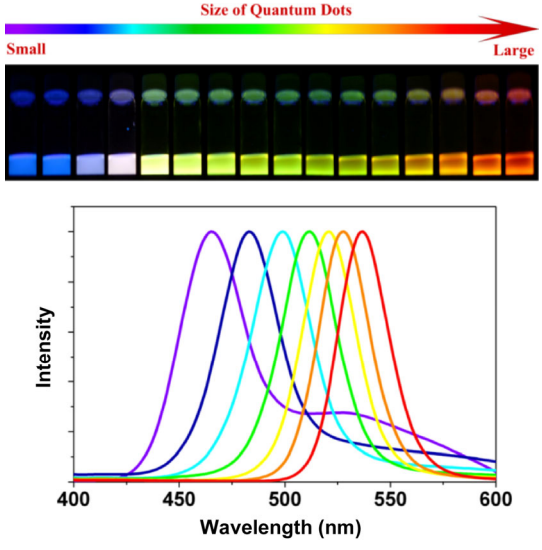

Fig. 9 The range of photoluminescence (PL) emission colour with size for CdSe QD from small to large, blue to red respectively, using a near-ultraviolet lamp with QD size from ~1 nm to ~10 nm (Bera et al. 2010)

Goldschmidt et al. (2009) presented a 4 cm^2 LSC system with a geometric concentration ratio of 0.8, which comprised of a stack of two plates doped with different types of dye (BA241 and BA856) and four GalnP solar cells at the edges. The system exhibited a collection efficiency of 6.7% which was higher than that of a similar system with only one dye (BA241), 5.1%.

Currie et al. (2008) proposed a tandem system consisting of two glass substrates coated with thin films of different organic dyes, i.e., the top LSC was based on rubrene to collect blue and green light and the bottom LSC was based on Pt(TPBP) to collect red light. The power conversion efficiencies of CdTe and Cu (In,Ga)Se2 solar cells were increased from 11.1% and 13.8% to 11.9% and 14.5%, respectively when they were attached to the edges of the top LSC of the system.

Slooff et al. (2008) tested a 50 mm × 50 mm × 5 mm PMMA plate containing 0.003 wt.% CRS040 dye and 0.01 wt.% Red305 dye combined with a 97% diffuse reflector on the backside and 4 GaAs cells connected in parallel at the plate edges. A power conversion efficiency of 7.1% was reported, and an efficiency reduction by 26% was found when the diffuse backside reflector was absent.

Bomm et al. (2011) developed and characterized a CdSe core/multishell quantum dot-based LSC. The results showed that QDs were well dispersed in a plastic matrix with a quantum yield of 45%. Besides, Si and GaAs cells were added to the LSC's edges to measure the external quantum efficiency and power conversion efficiency, the latter of which was reported to be 2.8%.

Gallagher et al. (2007) tested 8 small-scale quantum dot solar concentrator (QDSC) devices to determine their fill factors and comparative concentrating factors. The latter parameter was calculated by comparing the developed samples against three reference samples: (a) a polyurethane mirrored perspex mould casted sample without QDs, (b) an unmirrored perspex mould casted polyurethane without QD sample with the same PV orientation as QDSC and (c) with PV cell perpendicular to the incident radiation PV cell. Without exception, comparative concentrating factors were observed from a minimum of 1.33 to a maximum of 3.05 compared to sample (a) and higher values of comparative concentration factors were observed from 3.78 to 8.65 when compared to sample (b). Among the devices, Sample 5 (a QDSC of 0.08% volume fraction of CdSe/CdS F2 QD) attained the highest fill factor of 0.7, being 12.5% lower than that specified by the manufacturers for the PV cell.

Kerrouche et al. (2014) presented research into a stained glass window using 3D ray-tracing simulations to predict the transport of the trapped photons inside the LSC to the edge of the sheet to calculate power output and optical efficiency. Good agreement was reached between simulation

and experimental values with errors within 7%. The results showed that the optical power density collected at the prototype's edge reached the highest when the prototype was perpendicular to the light source. The prototype's optical efficiency was found to be in the range of 3%–6% for the tilt angle range of 0° to 85°, indicating the LSC window can generate energy from a wide range of incident light angles.

A prototype was presented by Fathi et al. (2017) incorporating an LSC coating on a window whereby the high energy photons from the Ultra Violet (UV) spectrum were recovered and shifted into the visible spectrum—collected by the PV cells attached at the window edges for electricity generation. The results showed that the device could produce 1.07 W/m^2 at low irradiance (250 W/m^2) and up to 4.28 W/m^2 in standard test conditions (1000 W/m^2). An average daily electricity generation of 450 Wh/day was estimated when installing the 20m^2 LSC glazing on typical houses in the North African site (Algiers).

3.3 Summary of BICPV glazing system studies

A wide variety of solar concentrator technologies, such as compound parabolic concentrator (CPC), Fresnel lens, and luminescent solar concentrator (LSC), have been proposed and developed (see Table 6) to reduce the PV material usage and improve the power conversion efficiency of BIPV modules. For building integration, solar concentrators with low geometric concentration ratios ($C_g < 4$) are recommended due to their wide acceptance angles allowing the collection of sunlight throughout the day without the need for mechanical sun-tracking systems. CPC systems are promising for BICPV applications, however, with some drawbacks like the PV cells overheating due to a large amount of concentrated solar energy on a small PV cell area. Hence further thermal performance assessments are required, and PV cooling strategies such as combination with air ventilation like double-skin façade or solar thermal collectors like PV/T systems can be adopted to solve the issue. LSCs based on fluorescent dyes and quantum dots also have a bright future, with numerous advantages such as wide angular acceptance range, aesthetic appearance, flat plate structure, simple fabrication process and low cost. On the other hand, more efforts need to be made to improve the optical efficiency of LSCs, for example, using wide-Stokes shift to minimise re-absorption losses (Mattiello et al. 2020). To design and optimise the solar concentrators performance, applying numerical tools such as ray-tracing software can obtain performance-related parameters such as optical efficiency and half-acceptance angle to be used as indicators to optimise the solar concentrators' structures, dimensions, and material properties. The optimised solar concentrators can be further evaluated for their electrical performance by I-V characterisation under indoor standard test conditions (viz. AM1.5, 1000 W/m^2 and 25 °C cell temperature) or outdoor environmental conditions. In addition, UV and temperature ageing tests are worthy to be conducted to evaluate the functionality and lifetime of solar concentrating optics, for example, transparent resin prototypes can suffer yellow discolouration and photodegradation after being used for several years (Abu-Bakar et al. 2015a).

4 Electricity-generating smart window systems

The application of smart windows can lead to the lower total energy consumption of buildings by controlling the solar heat and light transmitted through the windows into indoor spaces, with associated reduction in cooling, heating and/or electric lighting loads (Baetens et al. 2010). Compared with traditional windows, the interaction of smart windows with the internal and external environments can be complicated, thereby careful window design and pre-application research are imperative. Additionally, smart windows should fulfil aesthetic and economic requirements as part of the technical solution for producing net-zero energy buildings (Di Carlo et al. 2018).

Smart windows can be classified into two major types: active and passive. Active smart windows include electrochromic windows, suspended particle device (SPD) windows and polymer-dispersed liquid crystals (PDLC) windows, in which optical and thermal properties can be controlled by applying electrical stimuli as demanded

Table 6 Summary of relevant researches on BICPVs

Device name	Concentration type	PV cell	Power output	Quantum efficiency	Optical efficiency	Ref.
RACPC	Rotationally asymmetrical compound parabolic	Si-mono	0.050 W	n/a	84 %	Abu-Bakar et al. 2015b
PRIDE	truncated asymmetric compound parabolic concentrator	Si	70 W	n/a	>40 %	Mallick and Eames 2007
LSC/Qdot	CdSe core/multishell Qdots	Si, GaAs	—	45%	—	Bomm et al. 2011
LSC/Dye	Glazing with luminescent coating	mc-Si	4.8 W	>60 %	—	Fathi et al. 2017
LSC	Fluorescent concentrator	GaInP	580 mV	45%	—	Goldschmidt et al. 2009

by users (Casini 2018). Passive smart windows include thermochromic/ thermotropic windows and photochromatic windows, which autonomously respond with varying thermo-optical properties to temperature and light intensity, respectively (Casini 2018).

Smart windows can be integrated with PV cells to form hybrid solar windows, known as electricity-generating smart windows or optically switchable PV windows. There are two major configurations: (1) a stacked structure of PV layer, smart material layer and glass panes, and (2) mounting PV cells at the edges of a smart window. The sections below describe existing active and passive smart windows with integrated PVs, which can control daylight transmission and generate electricity onsite.

4.1 Active smart windows integrated with PV cells

Debije (2010) presented an energy-generating smart window consisting of a fluorescent-dye-doped liquid-crystal solution sandwiched between electrically conductive glass panels with PV cells mounted at the window edges, as shown in Figure 10. Such configuration realised the control of light transmission as well as power generation. In the light absorption (dark) mode, the fluorescent dyes which guested in the liquid crystals at a rest state absorbed incident light and re-emitted light at a longer wavelength, a fraction of which was trapped in the window by total internal reflection and collected by the edge-attached PV cells. In the light transmission (bright) mode, an external voltage was applied on the electrically conductive glass panels to change the tilt angle of the liquid crystals and fluorescent guest molecules, consequently, allowing more light to pass through the window into the room beyond. The results showed that the light absorption by the K160-type fluorescent dyes with 0.5% concentration decreased by 31% when voltage was applied, whereas the usable light for power generation decreased by just 11%, which indicated an increased emission efficiency of the dyes when they were aligned more homeotropically. The results revealed that the smart window can generate electricity in both modes, with a small loss in electricity generation for a more significant decrease in light transmission when the window switched from the dark state to the bright state.

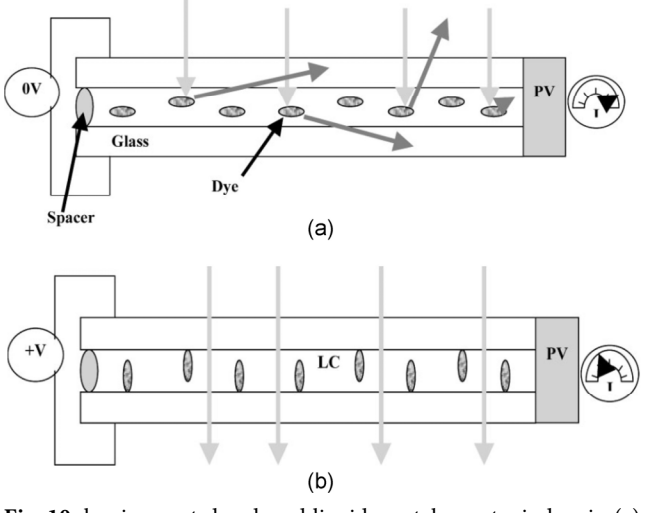

Fig. 10 luminescent-dye-doped liquid crystal smart window in (a) a light absorption mode and (b) a light transmission mode, with PV cells mounted at the window edges for electricity generation (Debije 2010; reprinted with permission ©2010 John Wiley and Sons)

Wang et al. (2012) developed an energy storage smart window (ESS) comprised of a supercapacitor and electrochromism function integrated by polyaniline nanowire arrays (electrodes). The addition of a solar cell permits the device to harness, store and use generated energy efficiently. When the sunlight is strong, the window darkens and blocks the sunlight from entering the internal space which is instead converted into electricity and stored electrochemically in the window. When the stored energy runs low, the window lightens. The ESS window shows high stability as a supercapacitor and can be used as a power source for electricity-consuming devices such as LCD screens.

Huang et al. (2012) designed a device composed of a semi-transparent Si thin-film solar cell (Si-TFSC) substrate, an electrochromic solution and a transparent non-conductive substrate. The PV-electrochromic device is a self-powered smart glass with electricity supplied by the integrated solar cell. Upon receiving solar radiation, the monolithically integrated Si-TFSC module produces electricity, a fraction of which induces the redox reaction of the electrochromic solution promoting the colour change of the device. Figure 11 shows the reaction mechanism diagram and the photo of a PV-EC device with an active area of 5.5 × 5 cm^2 with Si-TFSC strips, each of which has an area of 5 × 0.5 cm^2. The photoelectric conversion properties of an individual Si-TFSC were measured: V_{oc} = 0.93 V, J_{sc} = 12.3 mA/cm^2, fill factor = 73.23 %, P_{max} = 20.94 mW and power conversion efficiency = 8.38%. Moreover, the device uses an anodic colouring *N,N,N′,N′*-tetramethyl-*p*-phenylenediamine (TMPD) solution with a transmittance change (ΔT%) of around 70% at 590 nm, with periods of 200 seconds for a complete darkening process but 160 min for a complete beaching process. The device can be connected to an external load via a DC/AC inverter or to a DC charge storage device, to use or store the direct current produced by the Si-TFSC.

Martina et al. (2017) proposed self-powered trifunctional glazing (i.e., electricity generation, illumination and dynamic solar control), composed of a 12 cm × 17 cm photo-electrochromic (PEC) device with a 10 cm × 8 cm transparent white organic light-emitting diode (OLED) in a

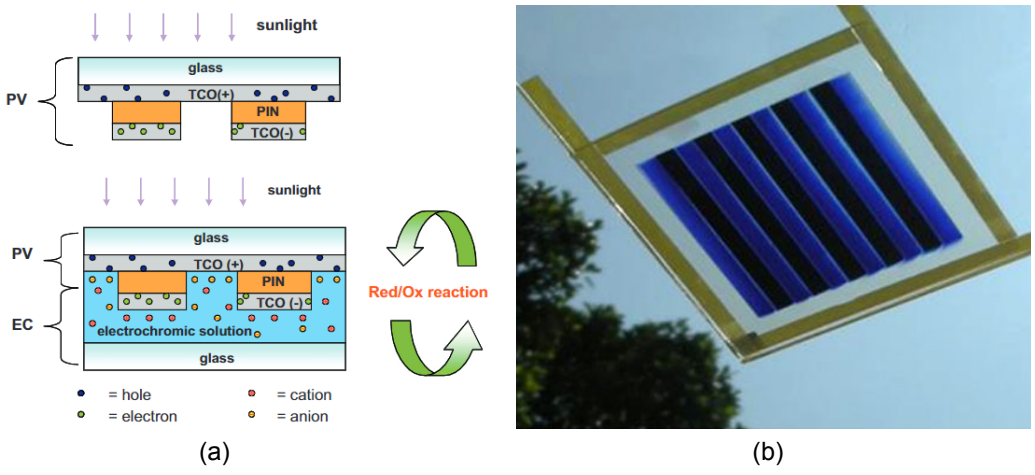

Fig. 11 (a) Sketch of the components and (b) photo of the proposed PV-EC device (Huang et al. 2012; reprinted with permission ©2012 Elsevier)

stacked configuration. The PEC device was manufactured with four dye-sensitized solar cells (DSSCs) and a central electrochromic section deposited on the same glass panel. The OLED was clamped onto the back of the PEC device to provide illumination at night. The generated energy was stored in supercapacitors, useful for inducing shading effects in the day or artificial lighting at night. The average efficiency of the four-dye sensitized solar cells was 2.4% and the transmittance modulation of the electrochromic section was 42% close to 700 nm, whilst coloration efficiency and modulation in optical density ΔOD reached maximums of 1.17 and 73 cm^2/C respectively near to 1200 nm.

Malara et al. (2014) developed a new structure for photovoltachromic windows, which consisted of three distinct electrodes (a transparent photoelectrode, a platinum electrode deposited on a PEN-ITO substrate and a WO3 electrode) with electrolytes filling the interspaces between the electrodes. This particular structure brings twofold benefits: self-powered fast-responsive control of the optical transmittance and production of electricity through solar energy conversion. The power conversion efficiencies of the samples with platinum active areas of 397, 360 and 320 mm^2 were measured to be 2.75%, 2.35% and 1.91% respectively, concluding that the larger the platinum area on the interposed Pt-ITO-PEN counter electrode, the higher the power conversion efficiency. It was also found that increasing the Platinum active area would slow down the bleaching process.

4.2 Passive smart windows integrated with PV cells

Kwon et al. (2015) developed a smart window by combining a photosensitive liquid crystal layer with a dye-sensitized solar cell in a stacked configuration. The liquid crystal layer switched to a clear state when exposed to UV radiation and to an opaque state when without a UV source. Different configuration types (from top to bottom) were evaluated by I-V characterisation under 1 sun condition (100 mW/cm^2): (1) DSSC-polarizer-LC-analyser structure (with J_{sc} = 16.43 mA/cm^2, V_{oc} = 0.744 V, fill factor = 0.626 and overall efficiency = 7.936%), (2) polarizer-LC-analyser-DSSC structure (with J_{sc} = 2.13 mA/cm^2, V_{oc} = 0.698 V, fill factor = 0.739, and efficiency = 1.099%) and (3) polarizer-DSSC-LC-analyser structure (with J_{sc} = 5.671 mA/cm^2, V_{oc} = 0.779 V, fill factor = 0.745 and efficiency = 3.248%). Type 2 had the poorest electrical performance because the DSSC was placed beneath the LC layer and received the least amount of incident light compared with the other two types. The smart window can be applied to building areas where privacy and security are required at night (opaque mode) and not in the daytime (clear mode).

A study from Guo et al. (2015) presented a smart photovoltaic window design comprised of a VO_2-nanoparticle thermochromic layer stacked on top of an organic solar cell, as shown in Figure 12. This window generates electricity utilising the visible solar radiation, whilst responding to ambient temperature changes by controlling the near-infrared (NIR) radiation entering the window. This device achieved a power conversion efficiency of 3.1%, with a solar modulation ability of 7.5% whilst maintaining visual transparency at 28.2%.

Zhou et al. (2013) reported a novel VO_2-based smart window with the dual functions of energy-saving and electricity generation. This window can regulate infrared transmittance and maintain visible transparency functioning as a normal thermochromic window, but with the additional ability to scatter and transport light to the edge-attached solar cells for power production. Three samples with different VO_2 layer structures were tested, named C_a (a combination of VO_2 particles deposited on a quartz plate),

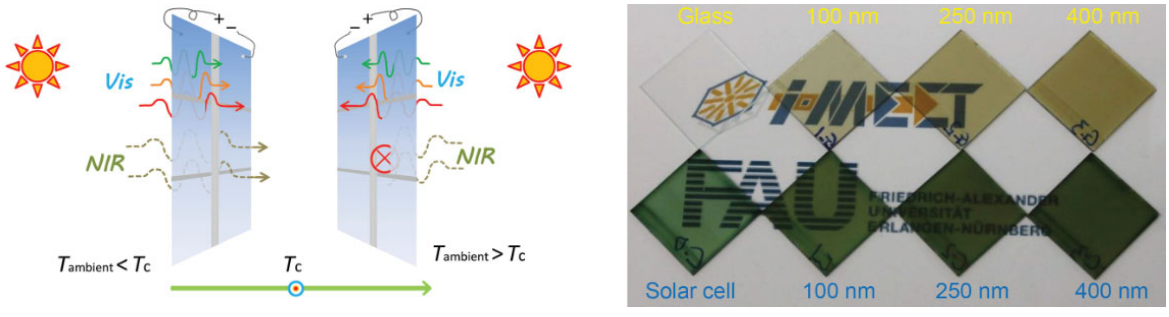

Fig. 12 (a) Working principle of the PV-thermochromic window; (b) photographs of clear glass substrates coated with VO_2 films of different thicknesses (first row) and organic PV glass coated with VO_2 films of different thicknesses (bottom row) (Guo et al. 2015; reprinted with permission ©2015 John Wiley and Sons)

C_b (a core-shell-shell structure consisting of VO_2, SIO_2 and TiO_2) and C_c (a combination of a smooth VO_2 thin film on a quartz plate). I-V characterization was conducted for the samples, C_a (with I_{sc} = 2.0 mA/cm^2, V_{oc} = 0.501 V, fill factor = 50.18% and efficiency = 0.50%), C_b (with I_{sc} = 1.74 mA/cm^2, V_{oc} = 0.498 V, fill factor = 59.68% and efficiency = 0.52%) and C_c (with I_{sc} = 1.32 mA/cm^2, V_{oc} = 0.497 V, fill factor = 52.06% and efficiency = 0.34%). By comparison, C_b had the highest values of power conversion efficiency and fill factor among the tested samples, indicating that the structure of C_b is more efficient in collecting scattered energy as compared to those of C_a and C_c.

4.3 Summary of electricity-generating smart window studies

Different from conventional clear and tinted windows with fixed colours and transparencies, smart windows such as electrochromic, photochemical and thermochromic windows can reversibly switch between a coloured state (with low transparency) and a bleached state (with high transparency) which occurs due to a change in environmental conditions such as electric field, light intensity and temperature. This dynamic behaviour can play a pivotal role in innovative building envelope designs that require adaptive control of daylight and solar heat gain in buildings. Integrating PV cells into a smart window is a ground-breaking idea, which makes simultaneous electricity generation and adaptive daylighting control possible. According to literature, electricity-generating smart windows can be manufactured by stacking a monolithic semi-transparent PV cell or multiple PV strips above or beneath an optically switchable layer that can be made from an active (e.g., electrochromic) or passive (e.g., thermochromic) smart material. In some designs such as self-powered PV-electrochromic devices, the electricity generated by the integrated PV cells can be stored and used to initiate and regulate the switching of the smart material, with no need for an external power supply. To attain good electricity generation rates, it is recommended to place PV cells on top of smart materials preventing the absorption of usable light. In addition, some drawbacks can be found depending on the technology used and need to be overcome in future attempts, such as low visible transparency, small solar modulation, long bleaching time, continuous electricity supply required to maintain the coloured/bleached state, material degradation and discolouration. Apart from the multi-layer stack designs, PV cells can be coupled to a smart window by mounting them at the glass edges. Such configuration allows the use of high-efficiency opaque PV cells such as crystalline silicon PV cells and has almost no effect on the window transparency. However, the electrical performance relies heavily on the light-scattering ability of the embedded smart material layer.

Although there have been a variety of studies investigating the optical and electrical characteristics of electricity-generating smart windows (see Table 7), there is still a lack of scientific evidence in the literature about the effectiveness of these window technologies in reducing building energy consumption and improving visual comfort. Therefore, a further in-depth research is required to fully assess the windows' characteristics and effects on building energy and daylight performance.

5 Discussion and recommendations for future development

Convectional PV window, more specifically conventional glass window integrated with PV cells, absorbs the incident sunlight and converts it into electricity, which in turn reduces the amount of light received by the indoor space and potentially improves the building energy efficiency and indoor comfort. However, its implementation is accompanied by several challenges, for example, a-Si PV windows have low power conversion efficiencies (up to 12% (Skandalos

Table 7 Highlights of smart window technologies and their main features

Smart window technology	Device description	Features	Power output	Transparency when activated	Ref.
Electrochromic-PV window	40 mm × 40 mm PET layer and Polyaniline electrode with Si PV cells	Self-powered, energy storage	—	30%	Wang et al. 2012
Electrochromic-PV window	20 mm × 20 mm window made of TiO_2, Pt, Pen/ITO and WO_3	Self-powered	—	—	Malara et al. 2014
Electrochromic-PV window	5.5 × 5 cm^2 Si thin-film solar cell substrate, an electrochromic solution, and a transparent non-conductive substrate	Control energy load and storage	20.94 mW	—	Huang et al. 2012
Electrochromic-PV window	All-printed 12 cm × 17 cm module, with DSSC, electrochromic area and 10 cm × 8 cm organic LED	Lighting and dynamic shading control	18.85 mW	30%	Martina et al. 2017
Thermochromic-PV window	100 nm, 250 nm and 400 nm thickness VO_2 films with an organic PV cell with an active area of 10.4 mm^2	NIR control	—	28. %	Guo et al. 2015

and Karamanis 2015)) and unnatural colours (brownish typically); DSSC windows can be manufactured in various colours but with cell degradation and efficiency reduction issues; c-Si PV windows have higher power conversion efficiencies (16%–22% (Skandalos and Karamanis 2015)), however not suitable for building areas where a uniform light distribution and unobstructed view are required. Integrating transparent concentrating optics such as dielectric CPCs into c-Si PV windows can increase the electric power output per unit cell area and thus reduce the usage of opaque c-Si PV cells (Sun et al. 2020) for better visual and aesthetic effects. A challenge for both conventional PV windows and CPV windows is that due to fixed thermo-optical properties, they cannot provide variable control of solar radiation transmission to meet the changing demands of buildings, i.e., solar shading in hot periods and passive solar heating in cold periods. Moreover, PV and CPV windows have to make compromises in the degree of visible transparency, when glare protection and enough daylight for the health and comfort of occupants are both required. Embedding smart materials with switchable visible and solar optical properties in PV windows can be a pragmatic solution to these challenges. Although a variety of electricity-generating smart windows such as PV-electrochromic and PV-thermochromic windows have been proposed (see Section 4), most of them have low values of power conversion efficiency (due to the use of thin-film solar cells such as a-Si and DSSC) and transparency (due to a multilayer stack structure with low-transparency PV and smart materials embedded). Furthermore, most of the previous research work has focused on presenting the working mechanisms and laboratory-measured properties of developed smart windows, with less emphasis on their performance on the building scale.

Thermotropic hydrogel materials have gained noticeable interest during the last decades for smart window applications. Thermotropic hydrogel-based smart windows have evolved with multifaceted characteristics by mixing different technologies and moving from the affinity intelligent window (AIW) concept developed by Watanabe (1998) to new complex solutions (Gyenes et al. 2003; Szilágyi et al. 2005; Wang et al. 2014a; Zhou et al. 2014). A new concept of PV-thermotropic smart windows was first introduced by Wu et al. (2016), and its feasibility has been demonstrated by Wu and his research team using simulation techniques in combination with experiments, including ray-tracing simulation for window geometry design and performance prediction (Wu et al. 2016; Liu and Wu 2021a, c), spectral analysis for material characterisation (Connelly et al. 2016; Connelly et al. 2017), building energy simulation (Allen et al. 2017), indoor and outdoor experiments (Liu and Wu 2021a, b).

Wu et al. (2016) presented a novel BICPV smart window featuring a multi-pane glazing with a thermotropic hydrogel layer and edge-attached solar cells. This window can provide onsite energy generation and react to ambient temperature changes by controlling the solar heat gains and daylighting levels in buildings, thus reducing the building energy consumption. The schematic concept of this novel device is shown in Figure 13. In a hot season, the proposed thermotropic layer switches to a translucent state and varies the proportions of the light transmitted through it and scattered from it depending on the amount of heat that is subjected to. Meanwhile, a proportion of the scattered light is directed through total internal reflection towards the optically coupled solar cells at the glass edges. In a cold season, the thermotropic layer has temperatures below a designed threshold switching temperature and appears transparent. That is, in summer the uncomfortably high solar irradiation which in conventional designs is blocked by shading devices and therefore lose heat to the environment will be collected by the proposed smart window to generate

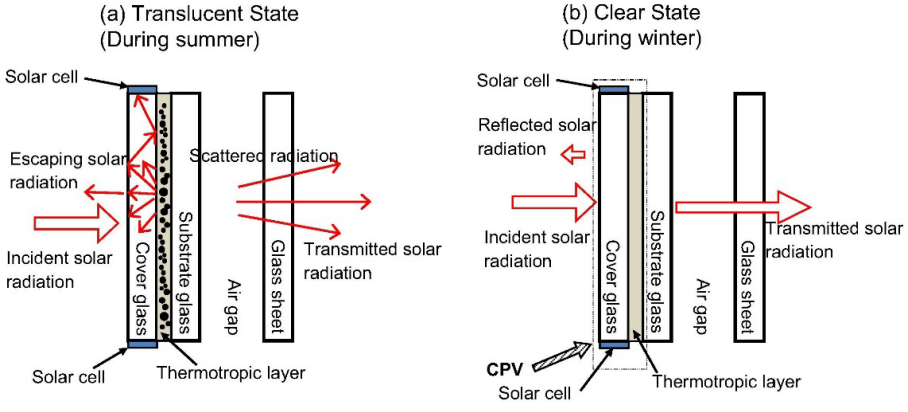

Fig. 13 (a) Light scattering state for electricity generation; (b) transparent state for indoor passive heating (Wu et al. 2016; reprinted with permission ©2016 Elsevier)

electricity; in winter, most of the incident light and heat are allowed to transmit through the system helping to offset heating and lighting energy demands.

The optical performance of the proposed BICPV smart window (C_g = 5) was presented in the study of Wu et al. (2016), where a module consisting of two 120 mm × 120 mm × 6 mm BK7 glazing covers, edge-attached solar cells and a thermotropic layer with dynamic reflectivity was modelled. No significant variation in the module's optical efficiency (ranging from 25% to 27.4%) was observed over the solar incidence angle range of −85° to 85°, indicating that the window has a wide angular acceptance range for the collection of direct and diffuse solar radiation, which is suitable for applications in Northern European climates. Subsequently, a larger-scale south-facing system with an aperture area of 1.44 m^2 consisting of 100 modules (i.e., each comprised two glazing covers of 120 mm × 120 mm × 6 mm and a thermotropic layer with 99% reflectivity) was modelled. The system's electrical performance was simulated in the climate of London with the input of realistic values of direct and diffuse solar radiation on 30th June 2014. The result showed that a maximum power output of 57 W can be generated by the system at 11:00 on the simulated day.

Presently, Connelly et al. (2016) developed a thermotropic membrane for the proposed BICPV smart window, which was synthesised of distilled water, hydroxypropyl cellulose (HPC) and gellan gum, as shown in Figure 14. The results showed that the 6 wt. % HPC hydrogel membrane sample had a switching temperature (T_s) of ~42 °C with a reduction of the average visible light transmittance from ~90% to ~20% and an increase of the average visible light reflectivity from ~10% to ~50% when the membrane was heated from 20 °C to 60 °C. Further work regarding the application of the HPC based smart window for dynamic control in a building was carried out by Allen et al. (2017). The visible and solar transmittances of the smart window integrated with a 6 wt.% HPC hydrogel membrane were 0.9 and 0.74 respectively when the membrane temperature was below the transition temperature of 40 °C and were 0.16 and 0.11 respectively when above the transition temperature. The smart window has a dynamic SHGC between 0.44 and 0.56, lower than the SHGC of traditional double glazing (0.74). A comparative simulation analysis was undertaken using EnergyPlus for the smart window with four different tilt angles (0°, 30°, 60° and 90°) installed in a typical cellular office at Palermo, Italy. The results showed that the outside ambient temperature and incident solar radiation play

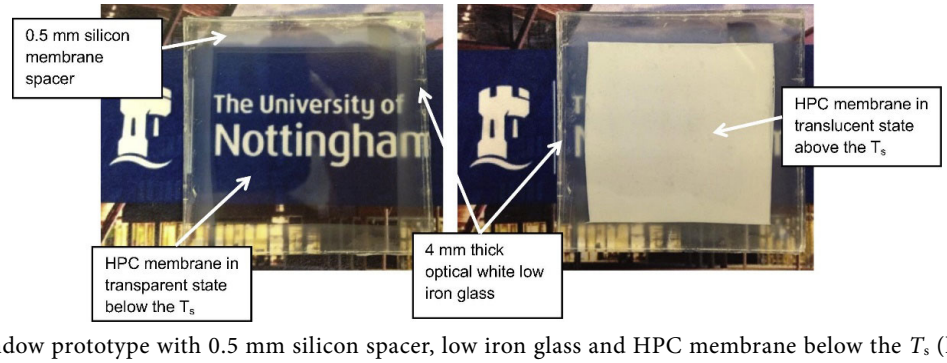

Fig. 14 Smart window prototype with 0.5 mm silicon spacer, low iron glass and HPC membrane below the T_s (left) and above the T_s (right) showing clear and light scattering states respectively (Connelly et al. 2016; reprinted with permission ©2016 Elsevier)

significant roles in the optical switching behaviour of the smart window. As for the horizontal skylight case (tilt angle = 0°), it was predicted that the HPC smart glazing can provide an annual energy saving of 22% compared to equivalent double glazing.

Liu and Wu (2021a, b, c) proposed a novel PV-thermotropic smart window, which consisted of crystalline-silicon solar cells encapsulated in an optical coating layer and stacked on top of an HPC based thermotropic hydrogel membrane, as shown in Figure 15. The thermotropic hydrogel was prepared by mixing HPC, sodium chloride and gelling agent in appropriate proportions to achieve a transition temperature of approximately 30 °C, visible transparency of over 90% in the clear state and solar modulation of approximately 76%. When the temperature of the thermotropic hydrogel membrane reached above 30 °C, it switched from a transparent state to a light-scattering state. This results in the reduction of solar heat and light entering the building space and the increase of electric power output from the solar cells due to the solar concentration effect shown in Figure 15(a). The smart window prototype was designed and preliminarily evaluated using a 3D ray-tracing technique and further evaluated by experiments under both indoor and outdoor environmental conditions. The results showed that the proposed smart window produced up to 12% higher maximum power output in its translucent state than a similar counterpart PV window with no thermotropic layer. Moreover, this PV-thermotropic smart window can autonomously change its visible light and solar transmittance (in the range of 10%–90%) depending on the levels of solar irradiation and ambient temperature, showing good potential in addressing overheating and glare issues.

Although the HPC based thermotropic hydrogels show good potential to improve the electricity generation and daylighting control capabilities of PV windows, their strong scattering and shielding in the visible light spectrum may affect the visual contact between the indoor and outdoor environments and increase the use of electric lighting to maintain desired luminance levels in interiors. Moreover, because the thermotropic hydrogels are made of biopolymer and natural gelling agents, their long-term functionality is a concern. Furthermore, the smart windows may encounter hydrogel leakage and drying problems, which place high demands on the sealing of the glazings. Future research is recommended to improve the solar-harvesting performance of the smart windows by taking all the spectrum-related factors into account, including the spectral properties of thermotropic hydrogels, the spectral response of solar cells, and indoor visual and thermal comfort. Future work is also needed to address the glazing sealing issues and material issues related to long-term stability (e.g., resistance to UV radiation and microorganisms) and weatherability (e.g., anti-freezing).

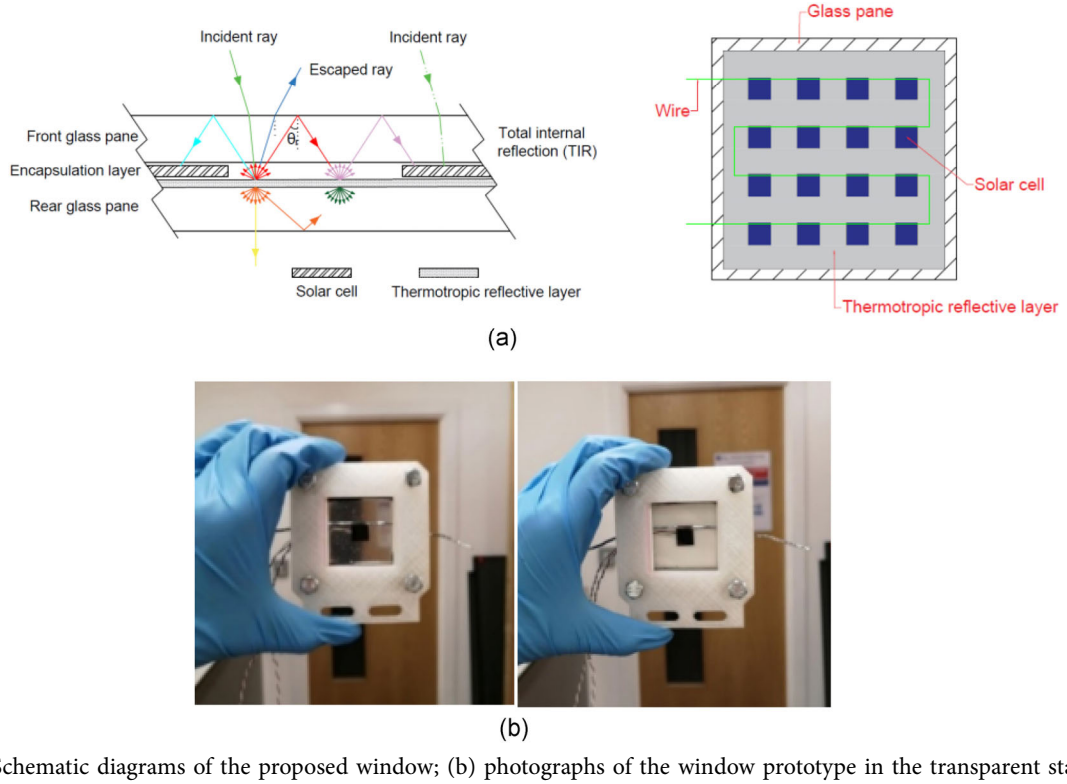

Fig. 15 (a) Schematic diagrams of the proposed window; (b) photographs of the window prototype in the transparent state (left) and light-scattering state (right) (Liu and Wu 2021a, b)

6 Conclusions

The introduction of new technologies to achieve zero-emission buildings has opened the door for the advanced windows development such as building integrated PV (BIPV), building integrated concentrating PV (BICPV) and electricity-generating smart windows. In the last decades, these technologies have evolved in different ways to suit the customers' needs and compete with conventional windows in terms of saving energy and improving visual comfort. This paper intends to provide a comprehensive review of well-established and emerging PV glazing technologies from working principles, previous research findings, optimisation methods, and future research opportunities perspectives.

The use of semi-transparent PVs (STPVs), such as a-Si and dye-sensitised solar cells, as part of building envelopes can serve to transmit daylight whilst providing electricity generation and some extent of solar shading and glare protection. However, a fundamental challenge is to achieve both high power conversion efficiency and transparency of an STPV at the same time. Alternatively, STPV glazings can be manufactured by employing high-efficiency PVs such as c-Si solar cells in narrow strips, which can probably improve the uniformity of indoor daylight distribution, viewing and aesthetics in comparison with traditional PV glazings that are typically made of large c-Si solar cells arranged in a square pattern. The influence of STPV glazings on building energy performance is mainly reflected in the reduction of cooling load but the increase of heating load, due to their relatively low SHGCs. Therefore, using STPV glazings can be beneficial for reducing the total energy consumption of buildings in cooling-dominated areas, but maybe not in cold climatic regions. In addition, the effect of STPV glazings varies depending on architectural design parameters such as WWR, orientation and inclination. A cost-effective approach to evaluate the applicability and energy-saving potential of STPV glazings which has been adopted in numerous studies is conducting building energy simulation with parametric analysis.

Apart from BIPV glazing applications, solar cells can be integrated onto shading devices such as venetian blinds with adjustable slat angles to generate electricity but also provide dynamic solar shading, or with solar thermal collectors in one system (PV/T) to efficiently convert solar energy into electricity and heat. The combination of PV glazings with solar concentrating devices represents a promising direction in improving the power conversion efficiency of BIPV glazing modules. Compound parabolic concentrators (CPCs) and variant designs (such as SEH and RACPC) with low geometric concentration ratios (≤ 4) are promising candidates for BICPV glazing applications, thanks to their high optical efficiencies and wide half-acceptance angles. However, despite effective solar concentration, these devices are subject to multiple problems that need to be solved, for example, efficiency loss due to cell overheating and non-uniform flux distribution on the cell surface, bulky structure and distorted view. In contrast with CPCs, luminescent solar concentrators (LSCs) could offer architects more degrees of design freedom, due to their ability to be manufactured in various degrees of transparency and colours, combined with the ability to collect both direct and diffuse solar radiation, planar shape and lightweight. Nonetheless, substantial efforts need to be made to improve the optical efficiency, spectral emission match with solar cells and environmental stability of LSCs.

Smart window integrated PV is an emerging technology that enables adaptive control of daylight transmission and electricity generation simultaneously. It can be constructed by laminating a monolithic semi-transparent PV with a layer of smart material (e.g., electrochromic material) or optically bonding PV cells around the edges of a smart window. In the latter configuration, the embedded smart material needs to be highly transparent in its clear state and highly scattering in its cloudy state, in order to achieve good daylighting, solar energy modulation and electrical performance. Thermotropic hydrogels consisting of hydroxypropyl cellulose biopolymer hold great potential for the application due to their strong light-scattering ability, large optical transmittance modulation, simple synthesis process and low cost, but need to be optimised in terms of long-term functionality.

Current researches on BICPV glazing and energy-generating smart window are oriented towards material development and window characterisation with less attention on their building integration. Future research is encouraged to assess developed window technologies on the building scale, to comprehensively understand their effects on building energy performance, indoor environmental conditions and comforts of occupants.

Acknowledgements

This work was supported by Consejo Nacional de Ciencia y Tecnología (CONACyT) through a PhD studentship awarded to Manlio Salas Castillo. This work was also supported by the Engineering and Physical Sciences Research Council, UK [grant number EP/S030786/1].

References

Abdallah M, El-Rayes K, Clevenger C (2015). Minimizing energy consumption and carbon emissions of aging buildings. *Procedia Engineering*, 118: 886–893.

Abu-Bakar SH, Muhammad-Sukki F, Freier D, et al. (2015a). Optimisation of the performance of a novel rotationally asymmetrical optical concentrator design for building integrated photovoltaic system. *Energy*, 90: 1033–1045.

Abu-Bakar SH, Muhammad-Sukki F, Freier D, et al. (2015b). Performance analysis of a novel rotationally asymmetrical compound parabolic concentrator. *Applied Energy*, 154: 221–231.

Abu-Bakar SH, Muhammad-Sukki F, Freier D, et al. (2016). Performance analysis of a solar window incorporating a novel rotationally asymmetrical concentrator. *Energy*, 99: 181–192.

Algora C, Rey-Stolle I (2016). Handbook of Concentrator Photovoltaic Technology. Chichester, UK: John Wiley & Sons.

Allen K, Connelly K, Rutherford P, et al. (2017). Smart windows—Dynamic control of building energy performance. *Energy and Buildings*, 139: 535–546.

Alrashidi H, Ghosh A, Issa W, et al. (2019). Evaluation of solar factor using spectral analysis for CdTe photovoltaic glazing. *Materials Letters*, 237: 332–335.

Aste N, Buzzetti M, del Pero C, et al. (2017). Visual performance of yellow, orange and red LSCs integrated in a smart window. *Energy Procedia*, 105: 967–972.

Baetens R, Jelle BP, Gustavsen A (2010). Properties, requirements and possibilities of smart windows for dynamic daylight and solar energy control in buildings: A state-of-the-art review. *Solar Energy Materials and Solar Cells*, 94: 87–105.

Baig H, Sarmah N, Chemisana D, et al. (2014a). Enhancing performance of a linear dielectric based concentrating photovoltaic system using a reflective film along the edge. *Energy*, 73: 177–191.

Baig H, Sellami N, Chemisana D, et al. (2014b). Performance analysis of a dielectric based 3D building integrated concentrating photovoltaic system. *Solar Energy*, 103: 525–540.

Baig H, Fernández EF, Mallick TK (2016). Influence of spectrum and latitude on the annual optical performance of a dielectric based BICPV system. *Solar Energy*, 124: 268–277.

Bak S, Kim D, Lee H (2016). Graphene quantum dots and their possible energy applications: a review. *Current Applied Physics*, 16: 1192–1201.

Barnham K, Marques JL, Hassard J, et al. (2000). Quantum-dot concentrator and thermodynamic model for the global redshift. *Applied Physics Letters*, 76: 1197–1199.

Bera D, Qian L, Tseng TK, et al. (2010). Quantum dots and their multimodal applications: A review. *Materials*, 3: 2260–2345.

Bomm J, Büchtemann A, Chatten AJ, et al. (2011). Fabrication and full characterization of state-of-the-art quantum dot luminescent solar concentrators. *Solar Energy Materials and Solar Cells*, 95: 2087–2094.

Bonilla JC, Bozkurt F, Ansari S, et al. (2016). Applications of quantum dots in Food Science and biology. *Trends in Food Science & Technology*, 53: 75–89.

Buker MS, Riffat SB (2015). Building integrated solar thermal collectors—A review. *Renewable and Sustainable Energy Reviews*, 51: 327–346.

Bunthof LAA, Kreuwel FPM, Kaldenhoven A, et al. (2016). Impact of shading on a flat CPV system for facade integration. *Solar Energy*, 140: 162–170.

Cabrera FJ, Fernández-García A, Silva RMP, et al. (2013). Use of parabolic trough solar collectors for solar refrigeration and air-conditioning applications. *Renewable and Sustainable Energy Reviews*, 20: 103–118.

Cannavale A, Hörantner M, Eperon GE, et al. (2017). Building integration of semitransparent perovskite-based solar cells: Energy performance and visual comfort assessment. *Applied Energy*, 194: 94–107.

Casini M (2016). Smart Buildings: Advanced Materials and Nanotechnology to Improve Energy-Efficiency and Environmental Performance. Oxford, UK: Elsevier.

Casini M (2018). Active dynamic windows for buildings: A review. *Renewable Energy*, 119: 923–934.

Chae YT, Kim J, Park H, et al. (2014). Building energy performance evaluation of building integrated photovoltaic (BIPV) window with semi-transparent solar cells. *Applied Energy*, 129: 217–227.

Chang H, Chen C-H, Kao M-J, et al. (2013). Photoelectrode thin film of dye-sensitized solar cell fabricated by anodizing method and spin coating and electrochemical impedance properties of DSSC. *Applied Surface Science*, 275: 252–257.

Chemisana D (2011). Building integrated concentrating photovoltaics: A review. *Renewable and Sustainable Energy Reviews*, 15: 603–611.

Chen F, Wittkopf SK, Khai Ng P, et al. (2012). Solar heat gain coefficient measurement of semi-transparent photovoltaic modules with indoor calorimetric hot box and solar simulator. *Energy and Buildings*, 53: 74–84.

Chen M, Zhang W, Xie L, et al. (2019). Experimental and numerical evaluation of the crystalline silicon PV window under the climatic conditions in southwest China. *Energy*, 183: 584–598.

Chopra KL, Paulson PD, Dutta V (2004). Thin-film solar cells: an overview. *Progress in Photovoltaics: Research and Applications*, 12: 69–92.

Chow TT (2010). A review on photovoltaic/thermal hybrid solar technology. *Applied Energy*, 87: 365–379.

Connelly K, Wu Y, Chen J, et al. (2016). Design and development of a reflective membrane for a novel Building Integrated Concentrating Photovoltaic (BICPV) 'Smart Window' system. *Applied Energy*, 182: 331–339.

Connelly K, Wu Y, Ma X, et al. (2017). Transmittance and reflectance studies of thermotropic material for a novel building integrated concentrating photovoltaic (BICPV) 'smart window' system. *Energies*, 10: 1889.

Cuce E, Riffat SB (2015). A state-of-the-art review on innovative glazing technologies. *Renewable and Sustainable Energy Reviews*, 41: 695–714.

Cuce E, Young CH, Riffat SB (2015). Thermal performance investigation of heat insulation solar glass: A comparative experimental study. *Energy and Buildings*, 86: 595–600.

Currie MJ, Mapel JK, Heidel TD, et al. (2008). High-efficiency organic solar concentrators for photovoltaics. *Science*, 321: 226–228.

Da Silva RM, Fernandes JLM (2010). Hybrid photovoltaic/thermal (PV/T) solar systems simulation with Simulink/Matlab. *Solar Energy*, 84: 1985–1996.

Davidsson H, Perers B, Karlsson B (2010). Performance of a multifunctional PV/T hybrid solar window. *Solar Energy*, 84: 365–372.

Davidsson H, Perers B, Karlsson B (2012). System analysis of a multifunctional PV/T hybrid solar window. *Solar Energy*, 86: 903–910.

Dayneko S, Lypenko D, Linkov P (2016). Application of CdSe/ZnS/CdS/ZnS core–multishell quantum dots to modern OLED technology. *Materials Today: Proceedings*, 3: 211-215.

Debije MG (2010). Solar energy collectors with tunable transmission. *Advanced Functional Materials*, 20: 1498–1502.

Delisle V, Kummert M (2014). A novel approach to compare building-integrated photovoltaics/thermal air collectors to side-by-side PV modules and solar thermal collectors. *Solar Energy*, 100: 50–65.

Di Carlo G, Biroli AO, Tessore F, et al. (2018). B-Substituted ZnII porphyrins as dyes for DSSC: a possible approach to photovoltaic windows. *Coordination Chemistry Reviews*, 358: 153–177.

Dimroth F, Grave M, Beutel P, et al. (2014). Wafer bonded four-junction GaInP/GaAs//GaInAsP/GaInAs concentrator solar cells with 44.7% efficiency. *Progress in Photovoltaics: Research and Applications*, 22: 277–282.

Dovzhenko D, Osipov E, Martynov I, et al. (2016). Porous silicon microcavity modulates the photoluminescence spectra of organic polymers and quantum dots. *Materials Today: Proceedings*, 3: 485–490.

Fathi M, Abderrezek M, Djahli F (2017). Experimentations on luminescent glazing for solar electricity generation in buildings. *Optik - International Journal for Light and Electron Optics*, 148: 14–27.

Fernández EF, Almonacid F, Sarmah N, et al. (2014). A model based on artificial neuronal network for the prediction of the maximum power of a low concentration photovoltaic module for building integration. *Solar Energy*, 100: 148–158.

Finetti C, Plavisch L, Chiari M (2016). Use of quantum dots as mass and fluorescence labels in microarray biosensing. *Talanta*, 147: 397–401.

First Solar (2014). First Solar builds the highest efficiency thin film PV cell on record. First Solar Press Release.

Fossa M, Ménézo C, Leonardi E (2008). Experimental natural convection on vertical surfaces for building integrated photovoltaic (BIPV) applications. *Experimental Thermal and Fluid Science*, 32: 980–990.

Gallagher SJ, Norton B, Eames PC (2007). Quantum dot solar concentrators: Electrical conversion efficiencies and comparative concentrating factors of fabricated devices. *Solar Energy*, 81: 813–821.

Goetzberger A, Greube W (1977). Solar energy conversion with fluorescent collectors. *Applied Physics*, 14: 123–139.

Goldschmidt JC, Peters M, Bösch A, et al. (2009). Increasing the efficiency of fluorescent concentrator systems. *Solar Energy Materials and Solar Cells*, 93: 176–182.

Goldschmidt JC (2012). Luminescent solar concentrator. In: Sayigh A (ed), Comprehensive Renewable Energy, Volume 1. Oxford, UK: Elsevier.

Gorgolis G, Karamanis D (2016). Solar energy materials for glazing technologies. *Solar Energy Materials and Solar Cells*, 144: 559–578.

Green MA, Emery K, Hishikawa Y, et al. (2015). Solar cell efficiency tables (Version 45). *Progress in Photovoltaics: Research and Applications*, 23: 1–9.

Green MA, Emery K, Hishikawa Y, et al. (2017). Solar cell efficiency tables (version 49). *Progress in Photovoltaics: Research and Applications*, 25: 3–13.

Guo F, Chen S, Chen Z, et al. (2015). Smart windows: printed smart photovoltaic window integrated with an energy-saving thermochromic layer (advanced optical materials 11/2015). *Advanced Optical Materials*, 3: 1479.

Gyenes T, Szilágyi A, Lohonyai T, et al. (2003). Electrically adjustable thermotropic windows based on polymer gels. *Polymers for Advanced Technologies*, 14: 757–762.

Haegel NM, Margolis R, Buonassisi T, et al. (2017). Terawatt-scale photovoltaics: Trajectories and challenges. *Science*, 356(6334): 141–143.

Hamers L (2017). Perovskites power up the solar industry. Available at https://www.sciencenews.org/article/perovskites-power-solar-industry

Hansen J, Sørensen H, Byström J, et al. (2018). Market, modelling, testing and demonstration in the framework of IEA SHC Task 35 on PV/thermal solar systems. In: Proceeding of 22nd European Photovoltaic Solar Energy Conference and Exhibition, Milan, Italy.

Hee WJ, Alghoul MA, Bakhtyar B, et al. (2015). The role of window glazing on daylighting and energy saving in buildings. *Renewable and Sustainable Energy Reviews*, 42: 323–343.

Heinstein P, Ballif C, Perret-Aebi L-M (2013). Building integrated photovoltaics (BIPV): Review, potentials, barriers and myths. *Green*, 3: 125-156.

Hoppe H, Sariciftci NS (2004). Organic solar cells: An overview. *Journal of Materials Research*, 19: 1924–1945.

Huang LM, Hu CW, Liu H, et al. (2012). Photovoltaic electrochromic device for solar cell module and self-powered smart glass applications. *Solar Energy Materials and Solar Cells*, 99: 154–159.

Ihara T, Gustavsen A, Jelle BP (2015). Effect of facade components on energy efficiency in office buildings. *Applied Energy*, 158: 422–432.

Ikkurti HP, Saha S (2015). A comprehensive techno-economic review of microinverters for Building Integrated Photovoltaics (BIPV). *Renewable and Sustainable Energy Reviews*, 47: 997–1006.

ITRPV (2014). International Technology Roadmap for Photovoltaic (ITRPV), 2013 Results.

ITRPV (2018). International Technology Roadmap for Photovoltaic (ITRPV), ITRPV Ninth Edition 2018 including maturity report.

Jäger-Waldau A (2004). Status of thin film solar cells in research, production and the market. *Solar Energy*, 77: 667–678.

Jayathissa P, Luzzatto M, Schmidli J, et al. (2017). Optimising building net energy demand with dynamic BIPV shading. *Applied Energy*, 202: 726–735.

Jean J, Brown PR, Jaffe RL, et al. (2015). Pathways for solar photovoltaics. *Energy & Environmental Science*, 8: 1200–1219.

Jelle BP, Breivik C (2012). State-of-the-art building integrated photovoltaics. *Energy Procedia*, 20: 68–77.

Jelle BP, Hynd A, Gustavsen A, et al. (2012a). Fenestration of today and tomorrow: A state-of-the-art review and future research opportunities. *Solar Energy Materials and Solar Cells*, 96: 1–28.

Jelle B, Breivik C, Drolsum Røkenes H (2012b). Building integrated photovoltaic products: A state-of-the-art review and future research opportunities. *Solar Energy Materials and Solar Cells*, 100: 69–96.

Jin Z, Owour P, Lei S, et al. (2015). Graphene, graphene quantum dots and their applications in optoelectronics. *Current Opinion in Colloid & Interface Science*, 20: 439–453.

Kalogirou SA (2004). Solar thermal collectors and applications. *Progress in Energy and Combustion Science*, 30: 231–295.

Kamat PV (2013). Quantum dot solar cells. The next big thing in photovoltaics. *The Journal of Physical Chemistry Letters*, 4: 908–918.

Kang M, Park NG, Park YJ, et al. (2003). Manufacturing method for transparent electric windows using dye-sensitized TiO_2 solar cells. *Solar Energy Materials and Solar Cells*, 75: 475–479.

Kang S, Hwang T, Kim JT (2012). Theoretical analysis of the blinds integrated photovoltaic modules. *Energy and Buildings*, 46: 86–91.

Kapsis K, Athienitis AK (2015). A study of the potential benefits of semi-transparent photovoltaics in commercial buildings. *Solar Energy*, 115: 120–132.

Kayes BM, Nie H, Twist R, et al. (2011) 27.6% Conversion efficiency, a new record for single-junction solar cells under 1 sun illumination. In Proceedings of the 37th IEEE Photovoltaic Specialists Conference, Seattle, WA, USA.

Kerrouche A, Hardy DA, Ross D, et al. (2014). Luminescent solar concentrators: From experimental validation of 3D ray-tracing simulations to coloured stained-glass windows for BIPV. *Solar Energy Materials and Solar Cells*, 122: 99–106.

Kessler J, Wennerberg J, Bodegard M, et al. (2003). Highly efficient Cu(In, Ga)Se mini-modules. *Solar Energy Materials and Solar Cells*, 75: 35–46.

Khairnar UP, Bhavsar DS, Vaidya RU, et al. (2003). Optical properties of thermally evaporated cadmium telluride thin films. *Materials Chemistry and Physics*, 80: 421–427.

Kim JJ, Jung SK, Choi YS, et al. (2010). Optimization of photovoltaic integrated shading devices. *Indoor and Built Environment*, 19: 114–122.

Krebs FC (2009). Fabrication and processing of polymer solar cells: A review of printing and coating techniques. *Solar Energy Materials and Solar Cells*, 93: 394–412.

Kroon JM, Bakker NJ, Smit HJP, et al. (2007). Nanocrystalline dye-sensitized solar cells having maximum performance. *Progress in Photovoltaics: Research and Applications*, 15: 1–18.

Kwon H-K, Lee K-T, Hur K, et al. (2015). Optically switchable smart windows with integrated photovoltaic devices. *Advanced Energy Materials*, 5(3): 1401347.

Lämmle M, Oliva A, Hermann M, et al. (2017). PVT collector technologies in solar thermal systems: A systematic assessment of electrical and thermal yields with the novel characteristic temperature approach. *Solar Energy*, 155: 867–879.

Lamnatou C, Chemisana D (2017). Concentrating solar systems: Life Cycle Assessment (LCA) and environmental issues. *Renewable and Sustainable Energy Reviews*, 78: 916–932.

Lechner P, Schade H (2002). Photovoltaic thin-film technology based on hydrogenated amorphous silicon. *Progress in Photovoltaics: Research and Applications*, 10: 85–97.

Lee JW, Park J, Jung H-J (2014). A feasibility study on a building's window system based on dye-sensitized solar cells. *Energy and Buildings*, 81: 38–47.

Lee TD, Ebong AU (2017). A review of thin film solar cell technologies and challenges. *Renewable and Sustainable Energy Reviews*, 70: 1286–1297.

Leite Didoné E, Wagner A (2013). Semi-transparent PV windows: A study for office buildings in Brazil. *Energy and Buildings*, 67: 136–142.

Li DHW, Lam TNT, Chan WWH, et al. (2009a). Energy and cost analysis of semi-transparent photovoltaic in office buildings. *Applied Energy*, 86: 722–729.

Li DHW, Lam TNT, Cheung KL (2009b). Energy and cost studies of semi-transparent photovoltaic skylight. *Energy Conversion and Management*, 50: 1981–1990.

Li X, Dai YJ, Li Y, et al. (2013). Comparative study on two novel intermediate temperature CPC solar collectors with the U-shape evacuated tubular absorber. *Solar Energy*, 93: 220–234.

Liao W, Xu S (2015). Energy performance comparison among see-through amorphous-silicon PV (photovoltaic) glazings and traditional glazings under different architectural conditions in China. *Energy*, 83: 267–275.

Linkov P, Krivenkov V, Nabiev I, et al. (2016). High quantum yield CdSe/ZnS/CdS/ZnS multishell quantum dots for biosensing and optoelectronic applications. *Materials Today: Proceedings*, 3: 104–108.

Liu C, Li B (2015). Multiple dyes containing luminescent solar concentrators with enhanced absorption and efficiency. *Journal of Optics*, 17: 025901.

Liu D, Sun Y, Wilson R, et al. (2020). Comprehensive evaluation of window-integrated semi-transparent PV for building daylight performance. *Renewable Energy*, 145: 1399–1411.

Liu X, Wu Y (2021a). Design, development and characterisation of a Building Integrated Concentrating Photovoltaic (BICPV) smart window system. *Solar Energy*, 220: 722–734.

Liu X, Wu Y (2021b). Experimental characterisation of a smart glazing with tuneable transparency, light scattering ability and electricity generation function. *Applied Energy*, 303: 117521.

Liu X, Wu Y (2021c). Monte-Carlo optical model coupled with Inverse Adding-Doubling for Building Integrated Photovoltaic smart window design and characterisation. *Solar Energy Materials and Solar Cells*, 223: 110972.

López CSP, Sangiorgi M (2014). Comparison assessment of BIPV facade semi-transparent modules: further insights on human comfort conditions. *Energy Procedia*, 48: 1419–1428.

Lu L, Law KM (2013). Overall energy performance of semi-transparent single-glazed photovoltaic (PV) window for a typical office in Hong Kong. *Renewable Energy*, 49: 250–254.

Makrides G, Zinsser B, Norton M, et al. (2010). Potential of photovoltaic systems in countries with high solar irradiation. *Renewable and Sustainable Energy Reviews*, 14: 754–762.

Malara F, Cannavale A, Carallo S, et al. (2014). Smart windows for building integration: A new architecture for photovoltachromic devices. *ACS Applied Materials & Interfaces*, 6: 9290–9297.

Mallick T, Eames P (2007). Design and fabrication of low concentrating second generation PRIDE concentrator. *Solar Energy Materials and Solar Cells*, 91: 597–608.

Manasrah A, Al Zyoud A, Abdelhafez E (2021). Effect of color and nano film filters on the performance of solar photovoltaic module. *Energy Sources, Part A: Recovery, Utilization, and Environmental Effects*, 43: 705–715.

Mangkuto RA, Rohmah M, Asri AD (2016). Design optimisation for window size, orientation, and wall reflectance with regard to various daylight metrics and lighting energy demand: a case study of buildings in the tropics. *Applied Energy*, 164: 211–219.

Manser JS, Christians JA, Kamat PV (2016). Intriguing optoelectronic properties of metal halide perovskites. *Chemical Reviews*, 116: 12956–13008.

Martina F, Pugliese M, Serantoni M, et al. (2017). Large area self-powered semitransparent trifunctional device combining photovoltaic energy production, lighting and dynamic shading control. *Solar Energy Materials and Solar Cells*, 160: 435–443.

Mattiello S, Sanzone A, Bruni F, et al. (2020). Chemically sustainable large stokes shift derivatives for high-performance large-area transparent luminescent solar concentrators. *Joule*, 4: 1988–2003.

Mattos LS, Scully SR, Syfu M, et al. (2012). New module efficiency record: 23.5% under 1-sun illumination using thin-film single-junction GaAs solar cells. In: Prceedings of th 38th IEEE Photovoltaic Specialists Conference (PVSC), 003187–003190.

Michael JJ, Iniyan S, Goic R (2015). Flat plate solar photovoltaic–thermal (PV/T) systems: A reference guide. *Renewable and Sustainable Energy Reviews*, 51: 62–88.

National Renewable Energy Laboratory (2017). Best research cell efficiency. Available at https://www.nrel.gov/pv/cell-efficiency.html.

Ng PK, Mithraratne N, Kua HW (2013). Energy analysis of semi-transparent BIPV in Singapore buildings. *Energy and Buildings*, 66: 274–281.

Nitz P, Hartwig H (2005). Solar control with thermotropic layers. *Solar Energy*, 79: 573–582.

Norton B, Eames PC, Mallick TK, et al. (2011). Enhancing the performance of building integrated photovoltaics. *Solar Energy*, 85: 1629–1664.

Ogbomo OO, Amalu EH, Ekere NN, et al. (2017). A review of photovoltaic module technologies for increased performance in tropical climate. *Renewable and Sustainable Energy Reviews*, 75: 1225–1238.

Olivieri L, Caamaño-Martín E, Moralejo-Vázquez FJ, et al. (2014). Energy saving potential of semi-transparent photovoltaic elements for building integration. *Energy*, 76: 572–583.

Parida B, Iniyan S, Goic R (2011). A review of solar photovoltaic technologies. *Renewable and Sustainable Energy Reviews*, 15: 1625–1636.

Park KE, Kang GH, Kim et al. (2010). Analysis of thermal and electrical performance of semi-transparent photovoltaic (PV) module. *Energy*, 35: 2681–2687.

Peng C, Huang Y, Wu Z (2011). Building-integrated photovoltaics (BIPV) in architectural design in China. *Energy and Buildings*, 43: 3592–3598.

Peng J, Curcija DC, Thanachareonkit A, et al. (2019). Study on the overall energy performance of a novel c-Si based semitransparent solar photovoltaic window. *Applied Energy*, 242: 854–872.

Polman A, Knight M, Garnett EC, et al. (2016). Photovoltaic materials: Present efficiencies and future challenges, *Science*, 352(6283): aad4424 .

Radut M, Mihai O (2015). Multifunctional Integrated photovoltaic window with advanced features of energy harvesting and indoor shading control: Hardware implementation. In: Proceedings of the 7th International Conference on Electronics, Computers and Artificial Intelligence (ECAI), Bucharest, Romania.

Ramanujam J, Bishop DM, Todorov TK, et al. (2020). Flexible CIGS, CdTe and a-Si: H based thin film solar cells: A review. *Progress in Materials Science*, 110: 100619.

Ramirez-Iniguez R, Deciga-Gusi J, Freier D, et al. (2017). Experimental evaluation of a solar window incorporating rotationally asymmetrical compound parabolic concentrators (RACPC). *Energy Procedia*, 130: 102–107.

Reisfeld R (2010). New developments in luminescence for solar energy utilization. *Optical Materials*, 32: 850–856.

Ruparathna R, Hewage K, Sadiq R (2016). Improving the energy efficiency of the existing building stock: A critical review of commercial and institutional buildings. *Renewable and Sustainable Energy Reviews*, 53: 1032–1045.

Sabry M, Eames PC, Singh H, et al. (2014). Smart windows: Thermal modelling and evaluation. *Solar Energy*, 103: 200–209.

Sahota L, Tiwari GN (2017). Review on series connected photovoltaic thermal (PVT) systems: Analytical and experimental studies. *Solar Energy*, 150: 96–127.

Sarmah N, Richards BS, Mallick TK (2011). Evaluation and optimization of the optical performance of low-concentrating dielectric compound parabolic concentrator using ray-tracing methods. *Applied Optics*, 50: 3303.

Sarmah N, Mallick TK (2015). Design, fabrication and outdoor performance analysis of a low concentrating photovoltaic system. *Solar Energy*, 112: 361–372.

Sellami N, Mallick TK, McNeil DA (2012). Optical characterisation of 3-D static solar concentrator. *Energy Conversion and Management*, 64: 579–586.

Sellami N, Mallick TK (2013). Optical characterisation and optimisation of a static Window Integrated Concentrating Photovoltaic system. *Solar Energy*, 91: 273–282.

Shanks K, Senthilarasu S, Mallick TK (2016). Optics for concentrating photovoltaics: Trends, limits and opportunities for materials and design. *Renewable and Sustainable Energy Reviews*, 60: 394–407.

Shen L-M, Liu J (2016). New development in carbon quantum dots technical applications. *Talanta*, 156–157: 245–256.

Singh H, Sabry M, Redpath DAG (2016). Experimental investigations into low concentrating line axis solar concentrators for CPV applications. *Solar Energy*, 136: 421–427.

Skandalos N, Karamanis D (2015). PV glazing technologies. *Renewable and Sustainable Energy Reviews*, 49: 306–322.

Skandalos N, Karamanis D (2016). Investigation of thermal performance of semi-transparent PV technologies. *Energy and Buildings*, 124: 19–34.

Slooff LH, Kinderman R, Burgers AR, et al. (2006). The luminescent concentrator illuminated. In: Proceedings of SPIE.

Slooff LH, Bende EE, Burgers AR, et al. (2008). A luminescent solar concentrator with 7.1% power conversion efficiency. *Physica Status Solidi (RRL) - Rapid Research Letters*, 2: 257–259.

Song JH, An YS, Kim SG, et al. (2008). Power output analysis of transparent thin-film module in building integrated photovoltaic system (BIPV). *Energy and Buildings*, 40: 2067–2075.

Spanggaard H, Krebs FC (2004). A brief history of the development of organic and polymeric photovoltaics. *Solar Energy Materials and Solar Cells*, 83: 125–146.

Späth M, Sommeling PM, van Roosmalen JAM, et al. (2003). Reproducible manufacturing of dye-sensitized solar cells on a semi-automated baseline. *Progress in Photovoltaics: Research and Applications*, 11: 207–220.

Stamatakis A, Mandalaki M, Tsoutsos T (2016). Multi-criteria analysis for PV integrated in shading devices for Mediterranean region. *Energy and Buildings*, 117: 128–137.

Stanisavljevic M, Krizkova S, Vaculovicova M, et al. (2015). Quantum dots-fluorescence resonance energy transfer-based nanosensors and their application. *Biosensors and Bioelectronics*, 74: 562–574.

Sukhanova A, Hafian H, Turini M, et al. (2016). Multiphoton imaging of tumor biomarkers *in situ* using single-domain antibodies conjugated with quantum dots in a set orientation. *Materials Today: Proceedings*, 3: 523–526.

Sun LL, Yang HX (2010). Impacts of the shading-type building-integrated photovoltaic claddings on electricity generation and cooling load component through shaded windows. *Energy and Buildings*, 42: 455–460.

Sun Y, Shanks K, Baig H, et al. (2018). Integrated semi-transparent cadmium telluride photovoltaic glazing into windows: Energy and daylight performance for different architecture designs. *Applied Energy*, 231: 972–984.

Sun Y, Liu D, Flor JF, et al. (2020). Analysis of the daylight performance of window integrated photovoltaics systems. *Renewable Energy*, 145: 153–163.

Szilágyi A, Gyenes T, Filipcsei G, et al. (2005). Thermotropic polymer gels: Smart gel glass. *Macromolecular Symposia*, 227: 357–366.

Tabish TA, Zhang S (2016). Graphene quantum dots: Syntheses, properties, and biological applications. In: Andrews D, Nann T, Lipson RH (eds), Comprehensive Nanoscience and Nanotechnology, 2nd edn. Oxford, UK: Elsevier.

Tavakoli MM (2016). Surface engineering of Pbs colloidal quantum dots using atomic passivation for photovoltaic applications. *Procedia Engineering*, 139: 117–122.

Tyagi VV, Kaushik SC, Tyagi SK (2012). Advancement in solar photovoltaic/thermal (PV/T) hybrid collector technology. *Renewable and Sustainable Energy Reviews*, 16: 1383–1398.

Ulavi T, Hebrink T, Davidson JH (2014). Analysis of a hybrid solar window for building integration. *Solar Energy*, 105: 290–302.

Ullal HS, Zwelbel K, Von Roedern B (1997). Current status of polycrystalline thin-film PV technologies. In: Proceedings of the 26th IEEE Conference on Photovoltaic Specialists, Anaheim, CA, USA.

van Sark WGJHM, Barnham KWJ, Slooff LH, et al. (2008). Luminescent Solar Concentrators—A review of recent results. *Optics Express*, 16: 21773.

van Sark WGJHM (2013). Luminescent solar concentrators—A low cost photovoltaics alternative. *Renewable Energy*, 49: 207–210.

Vanhoutteghem L, Skarning GCJ, Hviid CA, et al. (2015). Impact of facade window design on energy, daylighting and thermal comfort in nearly zero-energy houses. *Energy and Buildings*, 102: 149–156.

Volkov Y (2015). Quantum dots in nanomedicine: Recent trends, advances and unresolved issues. *Biochemical and Biophysical Research Communications*, 468: 419–427.

Wah WP, Shimoda Y, Nonaka M, et al. (2005). Field study and modeling of semi-transparent PV in power, thermal and optical aspects. *Journal of Asian Architecture and Building Engineering*, 4: 549–556.

Wang K, Wu H, Meng Y, et al. (2012). Integrated energy storage and electrochromic function in one flexible device: an energy storage smart window. *Energy & Environmental Science*, 5: 8384.

Wang M, Gao Y, Cao C, et al. (2014a). Binary solvent colloids of thermosensitive poly(N-isopropylacrylamide) microgel for smart windows. *Industrial & Engineering Chemistry Research*, 53: 18462–18472.

Wang W, Winkler MT, Gunawan O, et al. (2014b). Device characteristics of CZTSSe thin-film solar cells with 12.6% efficiency. *Advanced Energy Materials*, 4: 1301465.

Watanabe H (1998). Intelligent window using a hydrogel layer for energy efficiency. *Solar Energy Materials and Solar Cells*, 54: 203–211.

Weber WH, Lambe J (1976). Luminescent greenhouse collector for solar radiation. *Applied Optics*, 15: 2299.

Wei Y, Ebendorff-Heidepriem H, Zhao JT (2019). Recent advances in hybrid optical materials: integrating nanoparticles within a glass matrix. *Advanced Optical Materials*, 7: 1900702.

Wong PW, Shimoda Y, Nonaka M, et al. (2008). Semi-transparent PV: Thermal performance, power generation, daylight modelling and energy saving potential in a residential application. *Renewable Energy*, 33: 1024–1036.

Wu Y, Connelly K, Liu Y, et al. (2016). Smart solar concentrators for building integrated photovoltaic facades. *Solar Energy*, 133: 111–118.

Wu J, Zhang X, Shen J, et al. (2017). A review of thermal absorbers and their integration methods for the combined solar photovoltaic/thermal (PV/T) modules. *Renewable and Sustainable Energy Reviews*, 75: 839–854.

Xia J, Hong T, Shen Q, et al. (2014). Comparison of building energy use data between the United States and China. *Energy and Buildings*, 78: 165–175.

Xu S, Liao W, Huang J, et al. (2014). Optimal PV cell coverage ratio for semi-transparent photovoltaics on office building facades in central China. *Energy and Buildings*, 77: 130–138.

Yoo S-H, Lee E-T (2002). Efficiency characteristic of building integrated photovoltaics as a shading device. *Building and Environment*, 37: 615–623.

Yoon J-H, Song J, Lee S-J (2011a). Practical application of building integrated photovoltaic (BIPV) system using transparent amorphous silicon thin-film PV module. *Solar Energy*, 85: 723–733.

Yoon S, Tak S, Kim J, et al. (2011b). Application of transparent dye-sensitized solar cells to building integrated photovoltaic systems. *Building and Environment*, 46: 1899–1904.

Youssef AMA, Zhai ZJ, Reffat RM (2018). Generating proper building envelopes for photovoltaics integration with shape grammar theory. *Energy and Buildings*, 158: 326–341.

Zheng D, Zhao P, Zhu L (2019). Non-conjugated and π-conjugated functional ligands on semiconductive quantum dots. *Composites Communications*, 11: 21–26.

Zhou J, Gao Y, Zhang Z, et al. (2013). VO_2 thermochromic smart window for energy savings and generation. *Scientific Reports*, 3: 3029.

Zhou Y, Cai Y, Hu X, et al. (2014). Temperature-responsive hydrogel with ultra-large solar modulation and high luminous transmission for "smart window" applications. *Journal of Materials Chemistry A*, 2: 13550–13555.